

Figure 2. Quantitative estimation of *lacZ* gene expression in rat livers induced by intrabiliary and intraportal adenoviral administration. Recombinant adenoviruses (1×10^8 pfu/500 μ l) carrying the *lacZ* gene were infused retrogradely into the liver via the common bile duct or antegradely via the portal vein. Animals were sacrificed 4 days after adenoviral administration. Their livers were homogenized, and β -galactosidase activity in the liver was estimated by the chemiluminescent reporter gene assay. Livers of naïve rats that received no adenoviral administration were also subjected to the chemiluminescent assay to estimate background levels of β -galactosidase activity in normal rat livers. Each bar represents the mean \pm SD of 5 animals. CBD represents the common bile duct. *Indicates that the difference between the groups is statistically significant at $p < 0.001$.

activity in the liver induced by *lacZ* gene expression, X-gal staining was performed as described previously (22). Briefly, approximately half of the volume of the left-lateral hepatic lobe from each animal was fixed with 4% paraformaldehyde, 0.2% glutaraldehyde and 0.02% Nonidet P-40 in 0.1 M sodium phosphate buffer (pH 7.4) for 60 min at room temperature. Livers were then sliced into 50- μ m thick sections with a microslicer (DTK-3000; Dosaka EM, Kyoto, Japan). These slices were rinsed 3 times in PBS with 1 mM $MgCl_2$ and incubated overnight at 37°C in an X-gal (5-bromo-4-chloro-3-indolyl- β -galactosidase; Gibco, Grand Island, NY, USA) reaction mixture to detect *lacZ* gene expression.

Quantitative evaluation of β -galactosidase activity in the liver. To quantitatively measure the β -galactosidase activity in the liver induced by *lacZ* gene expression, a chemiluminescent reporter gene assay system using Galacton-Star (Tropix, Bedford, MA, USA) was used, as described previously (13). Briefly, approximately half the volume of the left-lateral hepatic lobe from each animal was homogenized in a lysis buffer consisting of 100 mM potassium phosphate (pH 7.8) and 0.2% Triton X-100. Liver homogenates were centrifuged at 10,000 rpm for 10 min at 4°C. Supernatants were collected, and 10 μ l of each supernatant sample was added to the reaction buffer containing the Galacton-Star chemiluminescent substrate. After incubation for 60 min at 37°C, β -galactosidase activity of the supernatant samples was measured using a luminometer (TR717 Microplate luminometer; Tropix). A standard curve was generated by serially diluting the reagent grade *Escherichia coli* β -galactosidase (G-5635; Sigma, St.

Louis, MO, USA) in lysis buffer. Protein concentrations of the supernatants were also measured using the Bio-Rad (Hercules, CA, USA) protein assay kit with bovine serum albumin as standard. β -galactosidase activity of each sample was standardized based on the protein content of the supernatant.

Evaluation of adverse effects by adenoviral administration.

For evaluating the adverse effects of adenoviral administration into the liver via the common bile duct or via the portal vein, serum biochemical parameters including aspartate aminotransferase (AST), alanine aminotransferase (ALT), lactate dehydrogenase (LDH), total protein, albumin, total bilirubin (free and conjugated), creatinine and blood urea nitrogen (BUN) of each rat administered with adenoviruses (5×10^8 pfu contained in 500- μ l inoculum volume) retrogradely into the biliary tract or antegradely into the portal vein were measured 4 days after adenoviral infusion. For histological analysis of cytopathic effects caused by intrabiliary and intraportal adenoviral administration, the left-median hepatic lobe of each animal was removed, fixed in 10% buffered formalin, embedded in paraffin, and stained with hematoxylin and eosin. Naïve animals that had not received adenoviral administration were also sacrificed and examined biochemically and pathologically as normal controls. Each group consisted of 5 animals.

Statistics. Results are expressed as means \pm SD. Standard descriptive statistics, Student's t-test and Welch's t-test, were used according to the distribution of experimental values. A p-value < 0.05 was considered to indicate a significant difference between groups.

Results

Histochemical analysis of transgene expression in the liver induced by intrabiliary and intraportal adenoviral administration. To examine the efficiency of adenovirus-mediated gene transfer into the liver caused by intrabiliary and intraportal adenoviral administration, 5×10^8 pfu of Adex1CALacZ adenoviruses carrying the *lacZ* gene under the transcriptional control of the CAG promoter were infused retrogradely into the common bile duct and antegradely into the portal vein of rats. When animals received this amount of adenoviruses into the common bile duct or into the portal vein, no obvious signs of the treatment-related side effects, such as body weight loss, impaired activity, and dry and disheveled fur, were observed.

We first confirmed that no X-gal staining-positive areas were observed in livers of rats, which were not given any adenoviral infusion. Based on our previous study (10-12), we determined that peak *lacZ* gene expression in the liver induced by intravenous administration of recombinant adenoviruses occurred 2-7 days after administration. Therefore, we examined *lacZ* gene expression in the liver at day 4 after intrabiliary or intraportal adenoviral administration. X-gal staining of liver sections of animals that received retrograde intrabiliary adenoviral infusion revealed that considerable areas in the liver were blue from the staining (Fig. 1A). X-gal staining-positive cells were seen predominantly at periportal areas, known as Rappaport's zone 1, indicating that hepatocytes near the bile duct were infected with adenoviruses infused

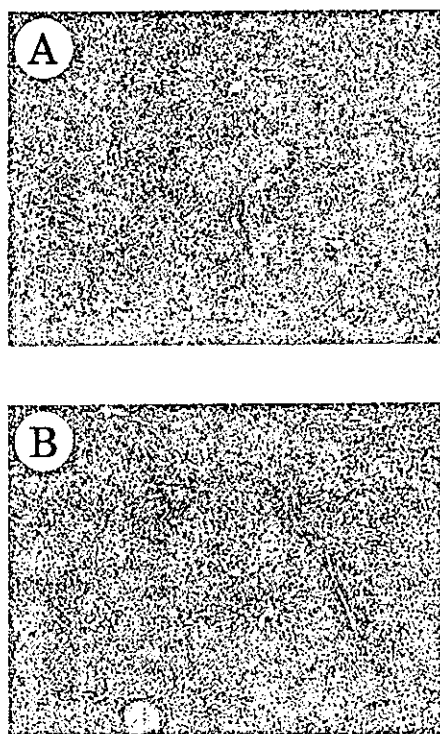


Figure 3. Histological analysis of the liver of animals that received intrabiliary or intraportal adenoviral administration. To examine the cytopathic effects of intrabiliary and intraportal adenoviral administration, livers were removed from rats and stained with hematoxylin and eosin when they were sacrificed 4 days after adenoviral administration. Histological analysis of liver sections from rats infused with adenoviruses into the common bile duct (A) and portal vein (B) revealed mild viral hepatitis-like pathological changes. Each group consisted of 5 animals. A representative picture is shown. Original magnification $\times 100$.

retrogradely into the common bile duct. However, a considerable number of hepatocytes expressing the *lacZ* gene were detected in lobular areas, the so-called zone 2 and a number of cells expressing the *lacZ* gene were also observed even in centrilobular areas, the so-called zone 3. Similar results were observed when the same amount of the same adenovirus was infused antegradely through the portal vein into the liver. At day 4 after adenoviral infusion into the portal vein, considerable areas in the liver were blue with X-gal staining (Fig. 1B). Although X-gal staining-positive cells were densely seen in zone 1, they spread from zone 1 to zone 2 and a considerable number of positive cells were also observed even at zone 3. Although it is difficult to accurately estimate the rate of cells expressing the *lacZ* gene in the liver, morphometric evaluation of liver sections using the public domain NIH Image Program (written by Wayne Rasband at the National Institutes of Health, Bethesda, MD, USA) revealed that approximately 30-40% of cells in the liver of animals infused intrabiliary with adenoviruses expressed the *lacZ* gene. Similarly, approximately 30-40% of cells were positive for X-gal staining in the liver of animals infused intraportally with adenoviruses.

Quantitative estimation of transgene expression in the liver induced by intrabiliary and intraportal adenoviral administration. To quantitatively estimate the efficiency of



Figure 4. Serum liver-related parameters of animals that received intrabiliary or intraportal adenoviral administration. To examine the toxic effects of intrabiliary and intraportal adenoviral administration, sera were collected from rats when they were sacrificed 4 days after adenoviral administration, and serum liver-related parameters were estimated. Each bar represents the mean \pm SD of 5 animals. CBD, ALT, AST and LDH represent the common bile duct, alanine aminotransferase, aspartate aminotransferase, lactate dehydrogenase, respectively. *Indicates that the difference between the groups is statistically significant at $0.01 < p < 0.05$.

gene transfer into the liver caused by intrabiliary and intraportal adenoviral administration, 5×10^8 pfu of Adex1CA1acZ adenoviruses were infused retrogradely into the common bile duct and antegradely into the portal vein of rats. Four days later, livers were homogenized and β -galactosidase activity of the homogenates was measured using the chemiluminescent reporter gene assay system. As shown in Fig. 2, levels of β -galactosidase activity in livers of naïve rats that did not receive adenoviral administration were quite low. Conversely, markedly high levels of β -galactosidase activity were detected in livers of animals that received retrograde intrabiliary and antegrade intraportal adenoviral administration, with values of $31,900 \pm 6,400$ and $34,700 \pm 5,100$ pg of β -galactosidase/mg protein, respectively. There were no significant differences in β -galactosidase activity between intrabiliary and intraportal adenoviral administration groups.

Cytopathic effects of adenoviral administration into the liver via intrabiliary and intraportal routes. Although retrograde intrabiliary and antegrade intraportal infusion of adenoviruses into rats did not cause any deaths or apparent side effects, it has been shown that intraportal and intravenous administration of adenoviruses provoked inflammation of the liver (3). Therefore, we pathologically examined the liver of animals that received adenoviral infusion into the liver via intrabiliary and intraportal routes. Animals were sacrificed and livers were removed 4 days after adenoviral administration. Histological analysis of liver sections of animals that received intrabiliary adenoviral administration revealed that mild viral hepatitis-like pathological changes such as mild infiltration of inflammatory cells predominantly at zone 1 and hyperplastic changes of hepatocytes (Fig. 3A). Similar pathological changes were also observed in the liver of animals that received intraportal adenoviral administration (Fig. 3B). These results indicate that although mild

hepatitis-like changes were caused in the liver not only by intrabiliary, but also by intraportal adenoviral administration, cytopathic effects examined histologically were not substantial.

We then biochemically examined side effects caused by adenoviral administration by measuring serum biochemical parameters including liver-related ones. As shown in Fig. 4, although serum levels of LDH were significantly elevated in animals treated with intraportal adenoviral administration compared with naïve animals that were not given adenoviral administration, the values were not substantially different. Furthermore, serum levels of ALT and AST, the most important liver-related parameters that reflect hepatic damage, were not significantly higher in animals treated with adenoviruses than in naïve controls. Serum levels of other liver-related biochemical parameters, such as albumin and total bilirubin, in adenovirus-treated animals were not significantly different from those of naïve controls (data not shown). Serum levels of renal biochemical parameters, such as creatinine and BUN, were also not significantly different among the groups (data not shown).

Discussion

Because systemic administration of adenoviral vectors induces transgene expression predominantly in the liver due to their highly hepatotropic disposition, the current focus for the route of gene delivery is on intravenous, intra-arterial and intrahepatic routes. One other way to transfer therapeutic genes into the liver is via the route of the biliary tract. A gene of interest, which is infused retrogradely into the biliary tract, is supposed to be delivered to the liver. Importantly, retrograde infusion of adenoviral vectors is feasible in clinical settings by use of a non-invasive endoscopic method, namely endoscopic retrograde cholangiography. In the present study, to examine the feasibility of liver-directed gene therapy via the biliary route, we retrogradely infused adenoviruses carrying a reporter *lacZ* gene into the common bile duct, and compared the gene transduction efficiency and the safety with intraportal adenoviral administration. Histochemical and quantitative analyses of transgene expression demonstrated that intrabiliary adenoviral administration could induce transgene expression in the liver as efficiently as intraportal adenoviral administration. Furthermore, no substantial side effects were observed in animals that received intrabiliary adenoviral administration.

Successful administration of adenoviruses into the liver via the biliary tract has been shown already. Yang *et al* (23) have shown that administration of 6×10^{11} pfu of adenoviruses into common bile duct of rats resulted in transgene expression in all of the biliary epithelial cells as well as >80% of parenchymal hepatocytes. Peeters *et al* (24) have shown that the introduction of 5×10^9 pfu of adenoviruses into the biliary tract of mice induced efficient transgene expression in hepatocytes. Terao *et al* (25) have shown that administration of 1×10^{11} pfu of adenoviruses into the common bile duct of rats induced transgene expression in >30% of hepatocytes as well as in biliary epithelial cells. Sullivan *et al* (26) have administered 1×10^{12} pfu of adenoviruses into the common bile duct of a rhesus monkey and demonstrated that approximately 10% of hepatocytes as well as many biliary

epithelial cells expressed the transgene. In the present study, we infused only 5×10^8 pfu of adenoviruses carrying the *lacZ* gene retrogradely into the liver through the common bile duct. This adenoviral amount corresponds to 1/1200 and 1/200 of the adenoviral amounts used in the rat studies performed by Yang *et al* (23) and Terao *et al* (25), respectively. Nevertheless, efficient transgene expression was achieved in rat livers and approximately 30-40% of cells in the liver expressed the *lacZ* gene. Although cells expressing the transgene were observed predominantly in zone 1, a considerable number of cells expressing the transgene were also observed not only in zone 2, but also in zone 3. We have shown previously that when adenoviruses were administered into the portal or tail vein of rats, cells expressing the transgene were observed predominantly in zone 1 (11,12). Peeters *et al* (24) have also shown that the introduction of adenoviruses into the biliary tract or portal vein of mice led to similar patterns of transgene expression in the liver. These phenomena appear to be reasonable because adenoviruses administered into the biliary tract, tail or portal vein reached the liver through the biliary epithelium and portal epithelium, respectively, resulting in predominant transgene expression in zone 1 of the liver. Taken collectively, these results indicate that adenoviral administration into the biliary tract can induce efficient transgene expression in the liver. Furthermore, it was shown in the present study that adenovirus-mediated gene transfer into the liver by retrograde intrabiliary adenoviral administration did not cause any substantial side effects.

Our results demonstrated in the present study support the feasibility of administering recombinant adenoviruses to the human biliary tract by a relatively non-invasive approach, namely endoscopic retrograde cholangiography. This widely practiced procedure is relatively safe, with rare complications. In this procedure, the common bile duct is cannulated during endoscopic visualization of the papilla of Vater of the duodenum. In clinical practice, endoscopically-placed biliary cannulas are used to safely deliver radio-opaque contrast agents to the biliary tract, and this approach should be effective for the infusion of recombinant adenoviruses. It allows for retrograde infusion of adenoviruses while antegrade outflow can be limited by balloon-catheterization of the distal common bile duct. Furthermore, after the termination of adenoviral infusion, excessive adenoviruses are delivered immediately into the duodenum and excreted in the stool.

In conclusion, retrograde adenoviral administration into the biliary tract may be a clinically practical modality for inducing successful expression of therapeutic genes in the liver. Although more investigations should be performed to establish useful gene therapy with adenoviruses, our results support the feasibility of gene therapy by means of adenoviral vectors. Furthermore, the results demonstrated here may have important implications for efficacy considerations when adenoviral vectors are employed in clinical settings.

Acknowledgements

This work was supported in part by a Grant-in-Aid for Scientific Research (B-14370185) from the Japanese Ministry of Education, Culture, Sports, Science and Technology.

References

1. Strauss SE: Adenovirus infections in humans. In: *The Adenoviruses*. Ginsberg HS (ed). Plenum Press, New York, pp451-496, 1984.
2. Rosenfeld MA, Yoshimura K, Trapnell BC, Yoneyama K, Rosenthal ER, Dalemans W, Fukayama M, Bargon J, Stier LE, Stratford-Perricaudet L, Perricaudet M, Guggino WB, Pavirani A, Lecocq JP and Crystal RG: *In vivo* transfer of the human cystic fibrosis transmembrane conductance regulator gene to the airway epithelium. *Cell* 68: 143-155, 1992.
3. Zabner J, Couture LA, Gregory RJ, Graham SM, Smith AE and Welsh MJ: Adenovirus-mediated gene transfer transiently corrects the chloride transport defect in nasal epithelia of patients with cystic fibrosis. *Cell* 75: 207-216, 1993.
4. Crystal RG, McElvaney NG, Rosenfeld MA, Chu CS, Mastrangeli A, Hey JG, Brody SL, Jaffe HA, Eissa NT and Danel C: Administration of an adenovirus containing the human CFTR cDNA to the respiratory tract of individuals with cystic fibrosis. *Nat Genet* 8: 42-51, 1994.
5. Stratford-Perricaudet LD, Levrero M, Chasse JF, Perricaudet M and Briand P: Evaluation of the transfer and expression in mice of an enzyme-encoding gene using a human adenovirus vector. *Hum Gene Ther* 1: 241-256, 1990.
6. Jaffe HA, Danel C, Longenecker G, Metzger M, Setoguchi Y, Rosenfeld MA, Gant TW, Thorgeirsson SS, Stratford-Perricaudet LD and Perricaudet M: Adenovirus-mediated *in vivo* gene transfer and expression in normal rat liver. *Nat Genet* 1: 372-378, 1992.
7. Kay MA, Landen CN, Rothenberg SR, Taylor LA, Leland F, Wiehle S, Fang B, Bellinger D, Finegold M, Thompson AR, Read M, Brinkhous KM and Woo SL: *In vivo* hepatic gene therapy: complete albeit transient correction of factor IX deficiency in hemophilia B dogs. *Proc Natl Acad Sci USA* 91: 2353-5357, 1994.
8. Ishibashi S, Brown MS, Goldstein JL, Gerard RD, Hammer RE and Herz J: Hypercholesterolemia in low density lipoprotein receptor knockout mice and its reversal by adenovirus-mediated gene delivery. *J Clin Invest* 92: 883-893, 1993.
9. Kozarsky KF, McKinley DR, Austin LL, Raper SE, Stratford-Perricaudet LD and Wilson JM: *In vivo* correction of low density lipoprotein receptor deficiency in the Watanabe heritable hyperlipidemic rabbit with recombinant adenoviruses. *J Biol Chem* 269: 13695-13702, 1994.
10. Kuriyama S, Tominaga K, Kikukawa M, Nakatani T, Tsujinoue H, Yamazaki M, Nagao S, Toyokawa Y, Mitoro A and Fukui H: Inhibitory effects of human sera on adenovirus-mediated gene transfer into rat liver. *Anticancer Res* 18: 2345-2351, 1998.
11. Kuriyama S, Tominaga K, Kikukawa M, Tsujimoto T, Nakatani T, Tsujinoue H, Okuda H, Nagao S, Mitoro A, Yoshiji H and Fukui H: Transient cyclophosphamide treatment before intraportal readministration of an adenoviral vector can induce re-expression of the original gene construct in rat liver. *Gene Ther* 6: 749-757, 1999.
12. Kuriyama S, Tominaga K, Mitoro A, Tsujinoue H, Nakatani T, Yamazaki M, Nagao S, Toyokawa Y, Okamoto S and Fukui H: Immunomodulation with FK506 around the time of intravenous re-administration of an adenoviral vector facilitates gene transfer into primed rat liver. *Int J Cancer* 85: 839-844, 2000.
13. Nakatani T, Kuriyama S, Tominaga K, Tsujimoto T, Mitoro A, Yamazaki M, Tsujinoue H, Yoshiji H, Nagao S and Fukui H: Assessment of efficiency and safety of adenovirus mediated gene transfer into normal and damaged murine livers. *Gut* 47: 563-570, 2000.
14. Tsujinoue H, Kuriyama S, Tominaga K, Okuda H, Nakatani T, Yoshiji H, Tsujimoto T, Akahane T, Asada K and Fukui H: Intravenous readministration of an adenoviral vector performed long after the initial administration failed to induce re-expression of the original transgene in rats. *Int J Oncol* 18: 575-580, 2001.
15. Tominaga K, Kuriyama S, Yoshiji H, Deguchi A, Kita Y, Funakoshi F, Masaki T, Kurokohchi K, Uchida N, Tsujimoto T and Fukui H: Repeated adenoviral administration into the biliary tract can induce repeated expression of the original gene construct in rat livers without immunosuppressive strategies. *Gut* 53: 1167-1173, 2004.
16. Fang B, Eisensmith RC, Li XH, Finegold MJ, Shedlovsky A, Dove W and Woo SL: Gene therapy for phenylketonuria: phenotypic correction in a genetically deficient mouse model by adenovirus-mediated hepatic gene transfer. *Gene Ther* 1: 247-254, 1994.
17. Nakamura Y, Wakimoto H, Abe J, Kanegae Y, Saito I, Aoyagi M, Hirakawa K and Hamada H: Adoptive immunotherapy with murine tumor-specific T lymphocytes engineered to secrete interleukin 2. *Cancer Res* 54: 5757-5760, 1994.
18. Niwa H, Yamamura K and Miyazaki J: Efficient selection for high-expression transfectants with a novel eukaryotic vector. *Gene* 108: 193-199, 1991.
19. Miyake S, Makimura M, Kanegae Y, Harada S, Sato Y, Takamori K, Tokuda C and Saito I: Efficient generation of recombinant adenoviruses using adenovirus DNA-terminal protein complex and a cosmid bearing the full-length virus genome. *Proc Natl Acad Sci USA* 93: 1320-1324, 1996.
20. Graham FL and Prevec L: Manipulation of adenovirus vectors. In: *Methods in Molecular Biology*. Murray EJ (ed). The Humana Press, Clifton, NJ, pp109-128, 1991.
21. Kanegae Y, Makimura M and Saito I: A simple and efficient method for purification of infectious recombinant adenovirus. *Jpn J Med Sci Biol* 47: 157-166, 1994.
22. Kuriyama S, Yoshikawa M, Ishizaka S, Tsujii T, Ikenaka K, Kagawa T, Morita N and Mikoshiba K: A potential approach for gene therapy targeting hepatoma using a liver-specific promoter on a retroviral vector. *Cell Struct Funct* 16: 503-510, 1991.
23. Yang Y, Raper SE, Cohn JA, Engelhardt JF and Wilson JM: An approach for treating the hepatobiliary disease of cystic fibrosis by somatic gene transfer. *Proc Natl Acad Sci USA* 90: 4601-4605, 1993.
24. Pecters MJ, Patijn GA, Lieber A, Meuse L and Kay MA: Adenovirus-mediated hepatic gene transfer in mice: comparison of intravascular and biliary administration. *Hum Gene Ther* 7: 1693-1699, 1996.
25. Terao R, Honda K, Hatano E, Uehara T, Yamamoto M and Yamaoka Y: Suppression of proliferative cholangitis in a rat model with direct adenovirus-mediated retinoblastoma gene transfer to the biliary tract. *Hepatology* 28: 605-612, 1998.
26. Sullivan DE, Dash S, Du H, Hiramatsu N, Aydin F, Kolls J, Blanchard J, Baskin G and Gerber MA: Liver-directed gene transfer in non-human primates. *Hum Gene Ther* 8: 1195-1206, 1997.

Successful laparoscopic radiofrequency ablation of hepatocellular carcinoma adhered to the mesentery after transcatheter arterial embolization

KAZUTAKA KUROKOHCHI¹, TSUTOMU MASAKI¹, TAKASHI HIMOTO¹, AKIHIRO DEGUCHI¹, SEIJI NAKAI¹, HIROHITO YONEYAMA¹, SHUHEI YOSHIDA¹, YASUHIKO KIMURA¹, HIDEYUKI INOUE¹, FUMIHIKO KINEKAWA¹, AKIRA YOSHITAKE¹, KUNIHIKO IZUISHI², SEISHIRO WATANABE¹ and SHIGEKI KURIYAMA¹

¹Third Department of Internal Medicine and ²First Department of Surgery, Kagawa University School of Medicine, 1750-1 Ikenobe, Miki-cho, Kita-gun, Kagawa 761-0793, Japan

Received August 10, 2004; Accepted October 4, 2004

Abstract. A 54-year-old male with hepatocellular carcinoma (HCC) underwent transcatheter arterial embolization (TAE) at a nearby hospital. He was then referred to our hospital for the purpose of additional treatment of HCC. Because TAE was not a complete therapy and HCC was growing and protruding from the left lobe of the liver, laparoscopic radiofrequency ablation (RFA) was chosen for the treatment of HCC. After inserting a laparoscope into the abdominal cavity, it was observed that HCC unexpectedly adhered to the mesentery as a result of TAE performed previously. After cutting off the adhered mesentery and removing it from the tumor, the combination therapy of percutaneous ethanol injection and RFA (PEI-RFA), developed at our department, was performed on the tumor. The tumor was successfully abrogated by PEI-RFA and the sufficient safety margin was confirmed by computed tomography after the treatment.

Introduction

Hepatocellular carcinoma (HCC) is one of the most serious malignancies worldwide. Tumor ablation technologies such as microwave, laser and radiofrequency have been shown to be reliable and effective for inducing thermally-mediated coagulation necrosis of primary HCC (1-4) and metastatic liver cancer (5,6). However, the effect of RFA is thought to be limited, and much effort has been made to enhance coagulated necrosis areas by the combination of RFA therapy

with other treatment modalities (7-15). Recently, we developed a novel combination therapy of percutaneous ethanol injection (PEI) and RFA (PEI-RFA) and reported that this combination therapy could induce larger coagulated necrosis without adverse events or much effort (16-18). Furthermore, we further developed this combination therapy under a laparoscopic approach for the treatment of HCC located on the surface of the liver and protruding from the liver. These kinds of tumors are thought to be difficult to treat under a percutaneous approach because of a high risk of bleeding from the tumor. We report here a rare case of HCC adhered to the mesentery after the treatment of TAE and successfully treated with laparoscopic PEI-RFA.

Case report

A 54-year-old male was referred to our hospital for the purpose of additional treatment of HCC located in the left lobe of the liver. He had a hepatitis C virus (HCV) infection in 1994 and received interferon (IFN) therapy for 24 weeks to eradicate HCV. However, the infected virus was not cleared by the IFN therapy, and the patient has not been thereafter followed-up with his liver function due to not attending the hospital for 9 years. He continued the habit of drinking 300 ml of Sake per day for >30 years. Because of the HCV infection and drinking habit, his hepatic reserve was impaired upon admission to our hospital. The laboratory data showing liver function and hepatic reserve were as follows: albumin, 2.7 g/μl; total bilirubin, 0.9 mg/dl; aspartate aminotransferase, 71 U/l; alanine aminotransferase, 52 U/l; platelet; 390,000/μl, hepaplastin test, 47%; prothrombin time, 57%. In November 2003, he went to a nearby hospital for blood examination and abdominal ultrasonography (US) because of general fatigue. A space-occupying lesion (SOL) of 2 cm in diameter was found in the S3 region of the left lobe of the liver. By dynamic computed-tomography (CT), this tumor showed enhancement in the early vascular phase and the defect in the late phase, resulting in the diagnosis of HCC. He underwent transcatheter arterial embolization (TAE)

Correspondence to: Dr Shigeki Kuriyama, Third Department of Internal Medicine, Kagawa University School of Medicine, 1750-1 Ikenobe, Miki-cho, Kita-gun, Kagawa 761-0793, Japan
E-mail : skuriyam@med.kagawa-u.ac.jp

Key words: hepatocellular carcinoma, laparoscopy, radiofrequency ablation, transcatheter arterial embolization, combination therapy, percutaneous ethanol injection

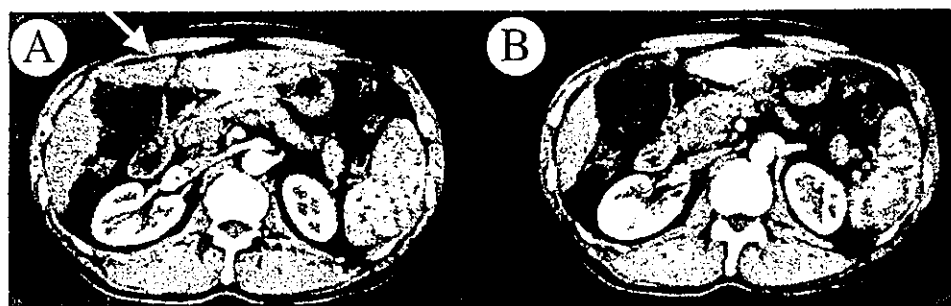


Figure 1. Contrast-enhanced CT (early phase) of HCC of the S3 region of the liver before the laparoscopic PEI-RFA. Lipiodol deposit was observed homogeneously in the entire region of the tumorous lesion. A tiny nodule showing the early enhancement was also detected on the surface of the S4 region of the liver (arrow).



Figure 2. The US echogram of the tumor of S3 region. The HCC was visualized as a round-shaped tumor and located immediately on the pancreas. A tiny HCC in the S4 region was not detected by the US before treatment.

for the treatment of HCC at the hospital before referral to our hospital. Dynamic CT taken at our hospital showed that lipiodol was homogeneously accumulated in the HCC located in the S3 region of the liver (Fig. 1A and B). Another tiny nodule showing early enhancement was also found on the surface of the S4 region of the liver (Fig. 1). Only the tumor in the S3 region was visualized as round-shaped by US (Fig. 2), and it was located immediately on the pancreas. The tiny tumor located in the S4 region could not be seen by US. Both tumors were present on the surface of the liver and TAE was not considered to be sufficient to destroy the tumorous region. Hepatic reserve was too impaired to receive an operative treatment, and ablation under a percutaneous approach was considered to be risky because the tumor was very close to the mesentery and the pancreas. Therefore, laparoscopic approach was chosen, and PEI-RFA, newly

developed at our department for enhancing the therapeutic effect, was adopted for the treatment of HCC. After inserting the laparoscope into the abdominal cavity, the lipiodol deposit was observed on the surface of the left lobe of the liver, but the deposit did not cover the whole area of the tumor and was observed as a spotty area (Fig. 3A). The tumor was lifted by a sound inserted from the right abdomen, and fine blood vessels from the mesentery flowing into the tumor were observed (Fig. 3B). Rapid-frozen sections prepared from the biopsy specimen taken from the surface of the tumor revealed the existence of viable HCC cells. HCC in the S4 region was also detected laparoscopically as a slightly protruding tumor from the surface of the liver (Fig. 3C). With regard to HCC in the S3 region, it appeared risky to ablate the tumor together with the adhered mesentery. Therefore, the adhered mesentery was cut off by the cutter (End GIA Universal, Surgical Company, USA) (Fig. 3D), and then the RFA electrode was firstly inserted into the center of the tumor, monitoring the depth of the inserted electrode by the linear type US. A 21-gauge PEI needle was inserted beside the electrode and 8 ml of ethanol (99.8%) was injected slowly into the tumor. Immediately after injection, RFA was started at 30 W, and the power output was stepwise increased to 80 W. Ablation was performed for a total of 13 min (Fig. 3E). During ablation, the tumor was constantly lifted by a sound to prevent the transmission of heat to the mesentery. It should be noted that no fluid containing tumor cells was spilled from the ablated tumor, indicating that the PEI-RFA developed at our department was a safe treatment modality even when performed by routine percutaneous approach. With ablation, the color of the tumor changed to yellow, and the tumor was atrophied by vaporization (Fig. 3E). Thereafter, relatively small-sized HCC located in the S4 region was also successfully treated with PEI-RFA (Fig. 3F). Abdominal dynamic CT taken after the operation clearly showed that the ablated region reached beyond the lipiodol deposit, and the area of safety margin was sufficiently obtained by laparoscopic PEI-RFA (Fig. 4).

Discussion

RFA technique has become the mainstream of non-surgical treatment modalities for liver tumor in clinical settings (3). To enhance the therapeutic effect, several innovations

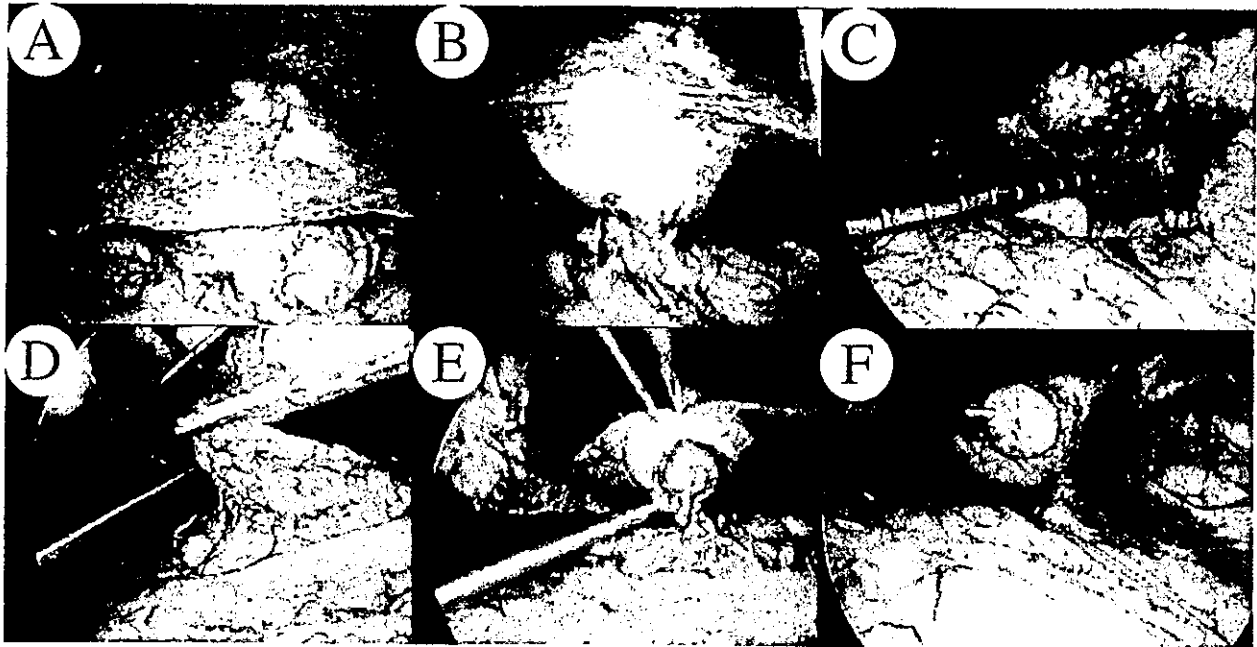


Figure 3. Laparoscopic observation of the tumor located on the surface of the S3 region (A) and S4 region (C). The spotted lipiodol deposit was observed on the surface of the tumor in the S3 region (A). The tumor of the S3 region was lifted by a sound inserted from the right abdomen, then the adhered mesentery under the tumor was also lifted, and fine blood vessels from the mesentery flowing into the tumor were observed (B). HCC of the S4 region was a tiny nodule and no lipiodol deposit was observed on the tumor. The adhered mesentery was cut off before PEI-RFA treatment (D). For HCC on the surface of the S3 region of the liver, a PEI needle was firstly inserted into the center of the tumor and the RFA electrode was inserted beside the PEI needle. Immediately after injecting a high concentration of ethanol (99.8%) through the PEI needle, RFA was performed. During ablation, the tumor was kept lifted by a sound to prevent the transmission of heat to the mesentery. The color of the tumor's surface changed from red and white to yellow (E). For HCC on the surface of S4 region, PEI-RFA was also performed. The color of the tumor changed from red to yellow, and the tumor was swollen during ablation (F).

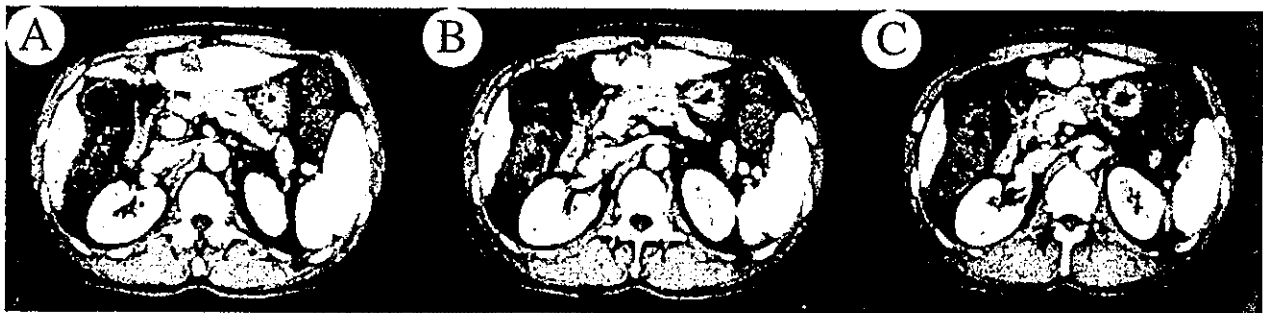


Figure 4. Contrast-enhanced CT of the tumors after treatment. The low density area around the lipiodol deposit of HCC (S3 region) was observed, indicating the safety margin area was obtained by laparoscopic PEI-RFA (A-C). The HCC on the S4 region was destroyed by treatment, and whole region of the tumor changed to the low density area (A).

have been attempted as additional treatments on RFA (9-12,15,20,21). We have developed a novel combination therapy of PEI-RFA and reported that this combination therapy was more effective than RFA alone for inducing largely-coagulated necrosis in human (16-18) and bovine livers (19). Recently, we applied this combination therapy to laparoscopic approaches, especially for HCC locating on the surface of the liver and protruding from the liver. These tumors are easy to access through a laparoscopic route. In addition, sufficient ablation under high power output control is possible, because laparoscopic PEI-RFA is done under general anesthesia, not a local one. In the case presented here, the tumor was located on the surface of the S3 and S4 regions of the liver and appeared to be good targets of

laparoscopic PEI-RFA. One extraordinary and interesting finding of this case was that the tumor unexpectedly adhered to the mesentery, probably due to the TAE performed previously. Furthermore, feeding fine blood vessels flowing from the mesentery into the adhered tumor were observed. To our knowledge, there are no reported cases with HCC that adhered to the mesentery after TAE, and this may be the first descriptive report of such HCC treated with PEI-RFA. If the tumor had not adhered to the mesentery, the treatment would have been performed more easily than the method done in the current study. Therefore, this case suggests that TAE may not necessarily be a good modality as a first-line treatment for tumors located on the surface of the liver and bordering the mesentery.

References

- Nagata Y, Hiraoka M, Akuta K, Abe M, Takahashi M, Jo S, Nishimura Y, Masunaga S, Fukuda M and Imura H: Radio-frequency thermotherapy for malignant liver tumors. *Cancer* 65: 1730-1736, 1990.
- Allgaier HP, Deibert P, Zuber I, Olschewski M and Blum HE: Percutaneous radiofrequency interstitial thermal ablation of small hepatocellular carcinoma. *Lancet* 353: 1676-1677, 1999.
- Goldberg SN, Gazelle GS, Solbiati L, Livraghi T, Tanabe KK, Hahn PF and Mueller PR: Ablation of liver tumors using percutaneous RF therapy. *Am J Roentgenol* 170: 1023-1028, 1998.
- Curley SA, Izzo F, Ellis LM and Nicholas Vauthey J: Radiofrequency ablation of hepatocellular cancer in 110 patients with cirrhosis. *Ann Surg* 232: 381-391, 2000.
- Solbiati L, Goldberg SN, Ierace T, Livraghi T, Meloni F, Dellanoce M, Sironi S and Gazelle GS: Hepatic Metastases: percutaneous radio-frequency ablation with cooled-tip electrodes. *Radiology* 205: 367-372, 1997.
- Solbiati L, Lerace T, Goldberg SN, Sironi S, Livraghi T, Fiocca R, Servadio G, Rizzato G, Mueller PR, Del Maschio A and Gazelle GS: Percutaneous US-guided radio-frequency tissue ablation of liver metastases: treatment and follow-up in 16 patients. *Radiology* 202: 195-203, 1997.
- Rossi S, Garbagnati F, Lencioni R, Allgaier H-P, Marchiano A, Fornari F, Quaretti P, Di Tolla G, Ambrosi C, Mazzaferro V, Blum HE and Bartolozzi C: Percutaneous radio-frequency thermal ablation of nonresectable hepatocellular carcinoma after occlusion of tumor blood supply. *Radiology* 217: 119-126, 2000.
- Buscarini L, Buscarini E, Di Stasi M, Quaretti P and Zangrandi A: Percutaneous radiofrequency thermal ablation combined with transcatheter arterial embolization in the treatment of large hepatocellular carcinoma. *Ultraschall Med* 20: 47-53, 1999.
- Yamasaki T, Kurokawa F, Shirahashi H, Kusano N, Hironaka K and Okita K: Percutaneous radiofrequency ablation therapy with combined angiography and computed tomography assistance for patients with hepatocellular carcinoma. *Cancer* 91: 1342-1348, 2001.
- Koda M, Murawaki Y, Mitsuda A, Oyama K, Okamoto K, Idobe Y, Suou T and Kawasaki H: Combination therapy with transcatheter arterial chemoembolization and percutaneous ethanol injection compared with percutaneous ethanol injection alone for patients with small hepatocellular carcinoma. *Cancer* 92: 1516-1524, 2001.
- Kitamoto M, Imagawa M, Yamada H, Watanabe C, Sumioka M, Satoh O, Shimamoto M, Kodama M, Kimura S, Kishimoto K, Okamoto Y, Fukuda Y and Dohi K: Radiofrequency ablation in the treatment of small hepatocellular carcinomas: comparison of the radiofrequency effect with and without chemoembolization. *Am J Roentgenol* 181: 997-1003, 2003.
- Livraghi T, Goldberg SN, Monti F, Bizzini A, Lazzaroni S, Meloni F, Pellicano S, Solbiati L and Gazelle GS: Saline-enhanced radio-frequency tissue ablation in the treatment of liver metastases. *Radiology* 202: 205-210, 1997.
- Honda N, Guo Q, Uchida H, Ohishi H and Hiasa Y: Percutaneous hot saline injection therapy for hepatic tumors: an alternative to percutaneous ethanol injection therapy. *Radiology* 190: 53-57, 1994.
- Burdio F, Guemes A, Burdio JM, Navarro A, Sousa R, Castiella T, Cruz I, Burzaco O, Guirao X and Lozano R: Large hepatic ablation with bipolar saline-enhanced radiofrequency: an experimental study in porcine liver with a novel approach. *J Surg Res* 110: 193-201, 2003.
- Hansler J, Frieser M, Schaber S, Kutschall C, Bernatik T, Muller W, Becker D, Hahn EG and Strobel D: Radiofrequency ablation of hepatocellular carcinoma with a saline solution perfusion device: a pilot study. *J Vasc Interv Radiol* 14: 575-580, 2003.
- Kurokohchi K, Watanabe S, Masaki T, Hosomi N, Funaki T, Arima K, Yoshida S, Miyauchi Y and Kuriyama S: Combined use of percutaneous ethanol injection and radiofrequency ablation for the effective treatment of hepatocellular carcinoma. *Int J Oncol* 21: 841-846, 2002.
- Kurokohchi K, Watanabe S, Masaki T, Hosomi N, Funaki T, Arima K, Yoshida S, Nakai S, Murota M, Miyauchi Y and Kuriyama S: Combination therapy of percutaneous ethanol injection and radiofrequency ablation against hepatocellular carcinomas difficult to treat. *Int J Oncol* 21: 611-615, 2002.
- Kurokohchi K, Masaki T, Miyauchi Y, Hosomi N, Yoneyama H, Yoshida S, Himoto T, Deguchi A, Nakai S, Inoue H, Watanabe S and Kuriyama S: Efficacy of combination therapies of percutaneous or laparoscopic ethanol-lipiodol injection and radiofrequency ablation. *Int J Oncol* 24: 1737-1743, 2004.
- Watanabe S, Kurokohchi K, Masaki T, Miyauchi Y, Funaki T, Inoue H, Himoto T, Kita Y, Uchida N, Touge T, Tatsukawa T and Kuriyama S: Enlargement of thermal ablation zone by the combination of ethanol injection and radiofrequency ablation in excised bovine liver. *Int J Oncol* 24: 279-284, 2004.
- Yasuda S, Ito H, Yoshikawa M, Shinozaki M, Goto N, Fujimoto H, Nasu K, Uno T, Itami J, Isobe K, Shigematsu N, Ebara M and Saisho H: Radiotherapy for large hepatocellular carcinoma combined with transcatheter arterial embolization and percutaneous ethanol injection therapy. *Int J Oncol* 15: 467-473, 1999.
- Okano H, Shiraki K, Inoue H, Ito T, Yamanaka T, Deguchi M, Sugimoto K, Sakai T, Ohmori S, Murata K, Takase K and Nakano T: Combining transcatheter arterial chemoembolization with percutaneous ethanol injection therapy for small size hepatocellular carcinoma. *Int J Oncol* 19: 909-912, 2001.

Genetic Polymorphisms Influencing Xenobiotic Metabolism and Transport in Patients With Primary Biliary Cirrhosis

Yasuhiko Kimura,^{1,2} Carlo Selmi,^{1,3} Patrick S. C. Leung,¹ Tin K. Mao,¹ Joseph Schauer,¹ Mitchell Watnik,⁴ Shigeki Kuriyama,² Mikio Nishioka,⁵ Aftab A. Ansari,⁶ Ross L. Coppel,⁷ Pietro Invernizzi,³ Mauro Podda,³ and M. Eric Gershwin¹

Epidemiological data suggest that environmental factors may trigger autoimmunity in genetically susceptible individuals. In primary biliary cirrhosis (PBC), it has been postulated that halogenated xenobiotics can modify self-molecules, facilitating the breakdown of tolerance to mitochondrial antigens. The transport and metabolism of xenobiotics is highly dependent on key genetic polymorphisms that alter enzymatic phenotype. We analyzed genomic DNA from 169 patients with PBC and 225 geographically and sex-matched healthy subjects for polymorphisms of genes coding for cytochromes P450 (CYPs) 2D6 (CYP2D6*4, CYP2D6*3, CYP2D6*5, and CYP2D6*6) and 2E1 (c1/c2), multidrug resistance 1 (MDR1 C3435T) P-glycoprotein, and pregnane X receptor (PXR C-25385T, C8055T, and A7635G). We compared the genotype frequencies in patients and controls and also correlated polymorphisms with PBC severity. The distributions of the studied genotypes did not significantly differ between patients and controls. However, when clinical characteristics of patients with PBC were compared according to genotype, the CYP2E1 c2 allele was associated with signs of more severe disease. **In conclusion**, genetic polymorphisms of CYP 2D6 and 2E1, PXR, and MDR1 do not appear to play a role in the onset of PBC. (HEPATOLOGY 2005;41:55–63.)

The etiology of primary biliary cirrhosis (PBC) remains elusive, but recent data suggest that the breaking of tolerance to the highly conserved 2-oxoacid dehydrogenase complex lipoylated domains of

the mitochondrial autoantigen could result from molecular mimicry initiated by an immune response directed toward xenobiotic structural analogues of lipoylated domains of the pyruvate dehydrogenase complex.¹ For example, sera from patients with PBC present antimitochondrial antibodies (AMAs) recognizing a number of synthetic structures that mimic a xenobiotic-modified lipoyl hapten conjugated to a peptide from the E2 subunit of the pyruvate dehydrogenase complex.² In addition, rabbits immunized with a xenobiotic (6-bromohexanoate) bovine serum albumin conjugate produce immunoglobulin G autoantibodies that react not only with xenobiotic but also self-reactive AMAs.³ Although many genetic factors conferring susceptibility to PBC have been suggested in population and family studies,^{4,5} no definitive genetic association with the onset of the disease or its outcome has yet been found. The liver is the primary organ involved in the metabolism and disposition of foreign chemicals. In such an environment, chemicals and/or their reactive metabolites may modify cellular proteins to form neoantigens.⁶ The recent findings of a possible role of molecular mimicry prompted us to determine whether polymorphisms in the genes involved in xenobiotic metabolism could contribute to the pathogenesis of

Abbreviations: PBC, primary biliary cirrhosis; CYP, cytochrome P450; MDR, multidrug resistance; PXR, pregnane X receptor; AMA, antimitochondrial antibody; SNP, single nucleotide polymorphism; PM, poor metabolizer; PGP, P-glycoprotein; PCR, polymerase chain reaction.

From the ¹Division of Rheumatology, Allergy and Clinical Immunology, University of California, Davis, CA; ²Third Department of Internal Medicine, School of Medicine, Kagawa University, Japan; ³Division of Internal Medicine, Department of Medicine, Surgery, and Dentistry, San Paolo School of Medicine, University of Milan, Italy; ⁴Statistical Laboratory, University of California, Davis, CA; ⁵Ehime Rousai General Hospital, Niihama City, Ehime Prefecture, Japan; ⁶Department of Pathology, Emory University School of Medicine, Atlanta, GA; and ⁷Department of Microbiology, Monash University, Clayton, Victoria, Australia.

Received April 24, 2004; accepted October 13, 2004.

Supported by National Institutes of Health grant 39588.

Y.K. and C.S. contributed equally to the study.

Address reprint requests to: M. Eric Gershwin, M.D., Division of Rheumatology, Allergy and Clinical Immunology, Genome and Biomedical Sciences Facility, University of California at Davis, 451 E. Health Sciences Drive, Suite 6510, Davis, CA 95616. E-mail: megershwin@ucdavis.edu; fax: 530-752-4669.

Copyright © 2004 by the American Association for the Study of Liver Diseases.

Published online in Wiley InterScience (www.interscience.wiley.com).

DOI 10.1002/hep.20516

Conflict of interest: Nothing to report.

Table 1. Characteristics of Patients With PBC at Time of Enrollment

	All Patients (n = 169)	PBC		P Value
		Early Disease (n = 77)	Advanced Disease (n = 92)	
Female sex (n)	153 (91%)	68 (88%)	85 (92%)	NS
Age at enrollment (yr)	62 ± 12	58 ± 12	66 ± 11	< .001
Disease duration (mo)	124 ± 72	90 ± 51	152 ± 75	< .001
AMA-positive (n)	139 (82%)	61 (79%)	78 (85%)	NS
Total bilirubin (mg/dL) (n.v. < 1.0)	1.6 ± 3.2	0.7 ± 0.35	2.4 ± 4.2	< .001
Albumin (g/dL) (n.v. >3.5)	4.2 ± 0.9	4.9 ± 0.7	3.7 ± 0.7	< .001
Prothrombin time (INR) (n.v. < 1.2)	1.04 ± .017	0.99 ± 0.08	1.08 ± 0.21	.001
With ascites (n)	22 (13%)	0	22 (24%)	< .001
Mayo score	5.7 ± 1.4	4.7 ± .07	6.5 ± 1.4	< .001

NOTE. Continuous variables are expressed as the mean ± SD.

Abbreviations: NS, not significant; INR, international normalized ratio; n.v., normal value.

PBC by genotyping a large population of patients with PBC and controls searching for a range of single nucleotide polymorphisms (SNPs). In particular, we decided to concentrate our efforts on mechanisms controlling the absorption of xenobiotics from the intestinal lumen, as well as their secretion into the bile (multidrug resistance 1 [MDR1]). Moreover, we were interested in analyzing the enzymes directly responsible for the metabolism of exogenous compounds (cytochromes P450 [CYPs]) or influencing the activity of the latter enzymes through regulation of their transcription (pregnane X receptor [PXR]).

Within the group of CYPs, CYP2D6 (debrisoquine/sparteine hydroxylase) is involved in the metabolism of approximately 20% of drugs.⁷ Several coding genetic polymorphisms have been identified that are associated with significant reduction of drug metabolism rates *in vivo* and *in vitro*; these are known as "poor metabolizers" (PMs).⁸ In particular, the PM phenotype is found in as many as 10% of Caucasian subjects⁹ and is most commonly due to the presence of null alleles for single base pair mutations (CYP2D6*3, CYP2D6*4, and CYP2D6*6, among others) or deletion of the whole gene (allele CYP2D6*5).⁷ As such, four alleles—CYP2D6*3, CYP2D6*4, CYP2D6*5, and CYP2D6*6—account for 93% to 97% of the PM phenotypes in Caucasians.¹⁰

CYP2E1 metabolizes several compounds, including ethanol, estrogenic metabolites, and halothane, and its activity is altered by nicotine.¹¹ These characteristics make this enzyme particularly interesting in PBC because of a striking female predominance.¹² Furthermore, PBC shares several characteristics (including the presence of serum AMAs) with halothane-induced hepatitis,¹³ and is diagnosed more commonly among smokers.¹⁴ A specific genetic polymorphism of CYP2E1 (*RsaI* restriction polymorphisms alleles c1/c2) has been widely investigated¹⁵ and is associated with reduced activity *per se*¹⁶ or altered

phenotype following interaction with specific compounds (e.g., ethanol or isoniazid), despite similar baseline activity.^{17,18}

The MDR1 gene encodes for the P-glycoprotein (PGP), a molecule that controls the cellular trafficking of substrates such as bilirubin and cancer drugs. In particular, PGP plays a role in excreting toxic xenobiotics and metabolites into the intestinal lumen as well as urine and bile. Although multiple mutations have been identified in MDR1, the exon 26 C3435T SNP is of special interest because of its association with a lower PGP expression in the intestine.¹⁹ It has also been suggested that the C3435T SNP might be associated with susceptibility to ulcerative colitis,²⁰ although the latter observation was not confirmed in another study.²¹

PXR is a nuclear receptor for steroid hormones and select xenobiotics whose activity regulates the expression of CYP3A4 and MDR1 in the liver and intestine. Importantly, there is an association of specific PXR SNPs with the CYP3A4 phenotype.²² We report the prevalence of CYP2D6*4, CYP2E1 c1/c2, MDR1 C3435T, and PXR (C-25385T, C8055T, A7635G) polymorphisms in patients with PBC and controls and have identified a correlation between CYP2E1 c1/c2 genotype and disease severity.

Patients and Methods

Patients. A total of 169 Italian patients with PBC who attended the Liver Unit at San Paolo Hospital (Milan, Italy) were enrolled in the study (Table 1). The diagnosis of PBC was based on internationally accepted criteria,^{23,24} and the AMA status of each patient was verified via indirect immunofluorescence. Of these 169 patients, 30 (18%) were AMA negative and 139 (82%) were AMA positive. All patients were negative for hepatitis B surface antigen and antibodies to hepatitis C virus and

denied alcohol abuse during the previous 12 months. The disease duration was calculated as the time between the date of the earliest recorded evidence of liver disease and the date of blood sampling. The latter evidence was determined through an extensive search of all laboratory data for alterations in cholestasis indicators (alkaline phosphatase > 1.5 normal values with or without altered γ -glutamyltransferase). All patients had undergone liver biopsy during the 12 months before blood sampling. Patients who did not have fibrosis according to liver histology (*i.e.*, Stages I-II according to Ludwig et al.²⁵) were considered to have early-stage PBC. Patients with liver fibrosis or cirrhosis (*i.e.*, Stages III-IV according to Ludwig et al.²⁵), patients who had a history of a major complication from cirrhosis (*e.g.*, ascites or gastrointestinal bleeding caused by portal hypertension), and patients who had undergone orthotopic liver transplantation for PBC were considered to have advanced-stage PBC. Advanced disease was found in 92 individuals (54.4%). Based on age, serum bilirubin and albumin, prothrombin time, and the presence of ascites, the Mayo score, the only validated prognostic index in PBC,²⁶ was calculated at the time of blood sampling or orthotopic liver transplantation. Two hundred twenty-five healthy subjects (blood donors) geographically and sex-matched with patients with PBC were used as a control population. Namely, 4 matched controls were obtained for every 3 patients. The study protocol followed the ethical guidelines of the most recent Declaration of Helsinki (Edinburgh, 2000); all patients provided written informed consent.

Genotyping. Whole blood samples were obtained from each patient and control and stored at -20°C before DNA extraction. DNA extraction was performed using a commercially available kit (Instagene Matrix; Bio-Rad Laboratories, Segrate, Italy). SNP genotypes were determined with polymerase chain reaction (PCR)/restriction fragment length polymorphism or the TaqMan SNP detection system (Applied Biosystems, Foster City, CA).

CYP2D6. CYP2D6*3 (2549A deletion) and CYP2D6*6 (1707T deletion) variants were analyzed using TaqMan-based methods. Amplification was performed using TaqMan universal master mix (Applied Biosystems) and 40X primers (forward 5'-CCTGACCCAGCTGGATGAG-3', reverse 5'-GCCAGGAAGGCTTAGT-3' for CYP2D6*3 and forward 5'-GGGCTGGGCAAGAAGTC-3', reverse 5'-CGAAGGCGGCACAAAGG-3' for CYP2D6*6) and allele-specific probes (VIC-ACTGAGCACAGGATGA-8NFQ, FAM-TAACTGAGCACGGATGA-8NFQ for CYP2D6*3 and VIC-CACCCACTGCTCCAG-8NFQ, FAM-TCACCCCTGCTCCAG-8NFQ for CYP2D6*6). PCR amplification included one cycle at 95°C for 10 min-

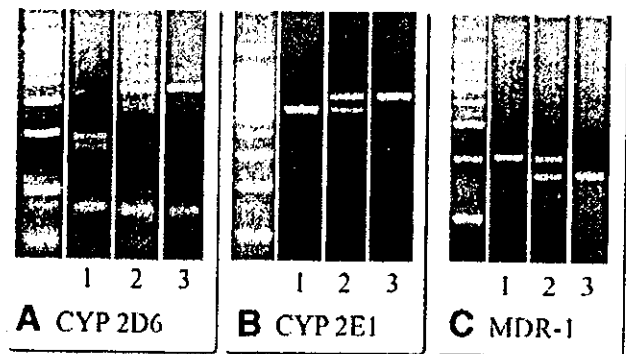


Fig. 1. Restriction fragment length polymorphism analysis of (A) CYP2D6 G1934A, (B) CYP2E1 c1/c2, and (C) MDR1 C3435T SNPs. PCR products of CYP2D6, CYP2E1, and MDR1 were digested with restriction enzymes *Bst*NI, *Rsa*I, and *Sau*3AI, respectively, and resolved via agarose gel electrophoresis. Restriction fragment patterns were scored as: (A) non-CYP2D6*4 homozygotes (77, 161, and 183 bp) in lane 1, heterozygous in lane 2, or CYP2D6*4 homozygous (77 and 344 bp) in lane 3; (B) CYP2E1 wild-type homozygous c1/c1 (360 and 50 bp) in lane 1, heterozygous c1/c2 in lane 2, or mutant-type homozygous c2/c2 (410 bp) in lane 3; and (C) MDR1 homozygous TT (197 bp) in lane 1, heterozygous CT in lane 2, or homozygous CC (158 and 39 bp) in lane 3. CYP, cytochrome P450; MDR, multidrug resistance.

utes followed by 40 cycles of 92°C for 15 seconds and 65°C for 1 minute. Allelic discrimination was performed on the post-PCR product by the 7900HT Sequence Detection System (Applied Biosystems). The presence of homozygosity for the CYP2D6*5 allele (deletion of the whole gene) was determined as described previously.²⁷

The CYP2D6 G1934A SNP (CYP2D6*4) was investigated as described by Brown et al.⁸ Briefly, using primer pairs 5'-GGTGTTCCTCGCGCGCTATG-3' and 5'-CTCGGTCTCTCGCTCCGCAC-3', DNA amplifications were performed with the PCR System 9700 (Applied Biosystems). PCR amplification consisted of an initial denaturation for 5 minutes at 94°C followed by 35 cycles of denaturation at 94°C for 1 minute, annealing at 60°C for 1 minute, and extension at 72°C for 1 minute. The terminal elongation was performed at 72°C for 7 minutes. PCR products were digested with restriction enzyme *Bst*NI (New England BioLab, Beverly, MA) overnight at 60°C , resolved in 3% agarose in Tris-acetate buffer, and visualized using ultraviolet ethidium bromide staining. Based on the pattern of the detected bands, restriction fragment patterns were scored as CYP2D6*4 homozygous (77 and 344 bp), non-CYP2D6*4 homozygous (77, 161, and 183 bp), or heterozygous (Fig. 1).

CYP2E1 c1/c2. CYP2E1 c1/c2 SNP was investigated as described by Choi et al.²⁸ Briefly, using primer pairs 5'-CCAGTCGAGTCTACATTGTCA-3' and 5'-TTCATTCTGTCTTCTAACTGG-3', DNA amplification was performed with an initial denaturation of 4 minutes at 94°C followed by 34 cycles at 94°C for 60

seconds, 60°C for 60 seconds, and 72°C for 60 seconds. The terminal elongation was performed at 72°C for 4 minutes. PCR products were digested with restriction enzyme *RsaI* (Invitrogen, Carlsbad, CA) at 37°C for 3 hours, resolved on 3% agarose gels in Tris-acetate buffer, and visualized with ethidium bromide staining. Based on the size of detected bands, samples were identified as either wild-type homozygous c1/c1 (360 and 50 bp), mutant-type homozygous c2/c2 (410 bp), or heterozygous c1/c2 (see Fig. 1).

MDR1 C3435T. The MDR1 C3435T SNP was determined as described by Cascorbi et al.²⁹ Briefly, using primer pairs 5'-TGTTTTTCAGCTGCTTGATGG-3' and 5'-AAGGCATGTATGTTGGCCTC-3', DNA amplification was performed with an initial denaturation of 2 minutes at 94°C followed by 35 cycles of 94°C for 30 seconds, 60°C for 30 seconds, and 72°C for 30 seconds. The terminal elongation was performed at 72°C for 7 minutes. PCR products were digested with restriction enzyme *Sau3AI* (New England BioLab) overnight at 37°C, resolved on 3.8% agarose gels in Tris-acetate buffer, and visualized with ethidium bromide staining. Based on the size of the detected bands, samples were identified as C/C homozygous (158 and 39 bp), T/T homozygous (197 bp), or heterozygous (Fig. 1).

PXR. Three PXR SNPs—C-25385 T, A7635G, and C8055T—were analyzed using a TaqMan-based method. Using the TaqMan universal master mix and 40× assay mix including primers and probes 5'-ACCACGATTGAGCAAACAGGTA-3', 5'-ACCTGAAGACAACCTGTG-GTCATT-3', VIC-TCCCAGGTTCTCTTTT-8NFQ, and FAM-TCCCAGGTTTTCTTTT-8NFQ (Assays-by-Design; Applied Biosystems), the PXR C-25385T SNP was determined. PCR amplification consisted of one cycle at 95°C for 10 minutes followed by 40 cycles of 92°C for 15 seconds and 65°C for 1 minute. Allelic discrimination was performed on the post-PCR product using the 7900HT Sequence Detection System (Applied Biosystems). Potentially, there were four clusters of points that corresponded to the three genotypes (CC, CT, TT) or to no amplification. Similarly, PXR A7635G SNP was analyzed using primers and probes 5'-CACAGTCATCCTCAGGGAAAGG-3', 5'-CAGCCATCCCATAATCCAGAAGT-3', VIC-CTC-TTCCTCTCACCCCA-8NFQ, and FAM-CTTC-CTCTCGCCCCA-8NFQ. PXR C8055T SNP was analyzed using primers and probes 5'-GGGATGATTA-GATCTTGTCAGCTT-3', 5'-CTGGAAGCCACCT-GTGGAT-3', VIC-CCCCTCCATCCTGTTAC-8NFQ, and FAM-CCCCTCCATTCTGTTAC-8NFQ'.

Statistical Analysis. Fisher exact tests were used for the analysis of categorical variables. In the case of continuous variables, the Mann-Whitney *U* test was used to

compare two groups, and the Kruskal-Wallis nonparametric one-way ANOVA was used to compare more than two groups. In the presence of statistically significant differences in categorical variables, odds ratios and 95% confidence intervals were calculated, and *P* values were corrected for age at enrollment and duration of disease. Statistical comparisons were made using Stata Statistical Software (Stata Corp., College Station, TX) or SAS (SAS Institute Inc., Cary, NC). All of the analyses were two-sided, and *P* values of less than .05 after correction were considered statistically significant.

Results

CYP2D6. The CYP2D6*4 allele frequencies in patients with PBC and controls are shown in Table 2. The obtained genotype frequencies corresponded to the Hardy-Weinberg equilibrium in our healthy Caucasian sample. Among 169 patients with PBC, 3 (2%) were found to be homozygous for the mutant allele (*4/*4), 118 (70%) were homozygous for the wild-type allele (N/N), and 48 (28%) were heterozygous (*4/N). No significant differences were observed between patients and controls in the frequencies of CYP2D6 genotypes. When the clinical characteristics of patients with PBC were analyzed according to the presence of the CYP2D6*4 allele (Table 3), no significant differences in genotype distributions were observed for age at enrollment, disease duration, or AMA status. Patients carrying the *4 allele presented signs of a slightly more advanced disease as indicated by higher prevalence of ascites (22% vs. 9%, *P* = .031 after correction for age and disease duration); higher but nonsignificant total bilirubin levels (2.2 ± 4.3 vs. 1.4 ± 2.7 ; *P* value not significant) were also observed. Moreover, the presence of the *4 allele was found to be associated with ascites (odds ratio, 2.76; 95% CI, 1.1-6.92). Data obtained from a preliminary study of CYP2D6*3 and CYP2D6*6 showed low allele frequencies in both patients (*n* = 90; 5/180 for CYP2D6*3 and 1/180 for CYP2D6*6) and controls (*n* = 90; 0/180 for CYP2D6*3 and 6/180 for CYP2D6*6). A similar preliminary study showed that homozygous CYP2D6*5 was not found in 80 patients with PBC and 80 controls. Based on these findings, further genotyping for these variants was not performed.

CYP2E1 c1/c2. The CYP2E1 genotype and allele frequencies among patients with PBC and controls are shown in Table 2. The obtained genotype frequencies corresponded to the Hardy-Weinberg equilibrium in our healthy Caucasian sample. 159 (94%) of 169 patients with PBC were found to be homozygous c1/c1 and 10 (6%) heterozygous c1/c2. No significant differences were observed between patients and controls in the frequencies of CYP2E1 genotypes.

Table 2. Distribution of CYP2D6, CYP2E1, and MDR1 Genotypes and Alleles in Patients With PBC and Controls

	Controls	PBC		
		Total	Early Disease	Advanced Disease
CYP2D6				
N/N	164/225 (73%)	118/169 (70%)	57/77 (74%)	61/92 (66%)
*4/N	57/225 (25%)	48/169 (28%)	19/77 (25%)	29/92 (32%)
*4/*4	4/225 (2%)	3/169 (2%)	1/77 (1%)	2/92 (2%)
*4 allele frequency	0.144	0.159	0.136	0.179
CYP2E1				
C1/C1	212/223 (95%)	159/169 (94%)	76/77 (99%)*	83/92 (90%)*
C1/C2	9/223 (4%)	10/169 (5%)	1/77 (1%)	9/92 (10%)
C2/C2	2/223 (1%)	0	0	0
C2 allele frequency	0.029	0.033	0.006	0.049
MDR1				
3435 C/C	60/225 (27%)	47/169 (28%)	23/77 (30%)	24/92 (26%)
3435 C/T	110/225 (49%)	88/169 (52%)	39/77 (51%)	49/92 (53%)
3435 T/T	55/225 (24%)	34/169 (20%)	15/77 (19%)	19/92 (21%)
T allele frequency	0.488	0.461	0.448	0.472

**P* = 0.043 after correction for age and disease duration; odds ratio 11.39 (95% CI 1.09-119.47) for c1/c2 genotype determining advanced disease.

When patients with PBC were analyzed according to disease stage, the frequency of the c1/c2 genotype was found to be significantly higher in advanced-stage PBC compared with early-stage PBC (*P* = .043 after correction for age and disease duration). Moreover, the presence of the c2 allele was found to be associated with advanced disease (odds ratio, 11.39; 95% CI, 1.09-119.47). When the clinical characteristics of patients with PBC were analyzed according to the presence of the c2 allele (Table 4), patients with this allele presented signs of more advanced disease as indicated by higher total bilirubin levels (3.6 ± 5.3 vs. 1.5 ± 3.0 ; *P* = .054), lower serum albumin levels (3.6 ± 0.9 vs. 4.3 ± 0.8 ; *P* = .036 after correction for age and disease duration), and higher Mayo score values (6.9 ± 1.9 vs. 5.6 ± 1.4 ; *P* = .015 after correction for age and disease duration).

MDR1 C3435T. The MDR1 C3435T genotypes and allele frequencies among patients with PBC and controls are shown in Table 2. The obtained genotype fre-

quencies corresponded to the Hardy-Weinberg equilibrium in our healthy Caucasian sample. Forty-seven (28%) of 169 patients with PBC were found to be homozygous C/C, 34 (20%) were homozygous T/T, and 88 (52%) were heterozygous C/T. No significant differences were observed between patients and controls in the frequencies of MDR1 genotypes. No significant differences in genotype distributions were observed between patients with early and advanced disease (T allele frequency 0.442 in early disease vs. 0.473 in advanced disease) nor in the clinical characteristics across the three genotypes (data not shown).

PXR. The PXR1 C-25385T genotypes and allele frequencies among patients with PBC and controls are shown in Table 5. The obtained genotype frequencies corresponded to the Hardy-Weinberg equilibrium in our healthy Caucasian sample. Seventy-two (43%) of 167 patients with PBC were found to be homozygous C/C, 24

Table 3. Clinical Features of Patients With PBC and the Presence of the CYP2D6*4 Allele

	N/N (n = 118)	*4/N + *4/*4 (n = 51)	P Value (Corrected)
Female sex (n)	106 (90%)	47 (92%)	NS
Age at enrollment (yr)	62 ± 13	62 ± 11	NS
Disease duration (mo)	122 ± 71	127 ± 76	NS
AMA-positive (n)	99 (84%)	40 (78%)	NS
Total bilirubin (mg/dL) (n.v. < 1.0)	1.4 ± 2.7	2.2 ± 4.3	.194
Albumin (g/dL) (n.v. > 3.5)	4.3 ± 0.9	4.2 ± 0.9	NS
Prothrombin time (INR) (n.v. < 1.2)	1.04 ± 0.18	1.03 ± 0.14	NS
Ascites (n)	11 (9%)	11 (22%)	.031 (.031)*
Mayo score	5.6 ± 1.4	5.9 ± 1.5	NS

NOTE. Continuous variables are expressed as the mean ± SD.

Only *P* values below .2 for the comparison between patient groups are reported before and after correction for age and disease duration.

*Odds ratio 2.76 (95% CI, 1.1-6.92) for *4 allele determining the presence of ascites.

Abbreviations: NS, not significant; INR, international normalized ratio; n.v., normal value.

Table 4. Clinical Features of Patients With PBC and the Presence of the CYP2E1 c2 Allele

	c1/c1 (n = 159)	c1/c2 (n = 10)	P Value (Corrected)
Female sex (n)	143 (90%)	10 (100%)	NS
Age at enrollment (yr)	62 ± 12	64 ± 13	NS
Disease duration (mo)	122 ± 69	155 ± 112	NS
AMA-positive (n)	131 (82%)	8 (80%)	NS
Total bilirubin (mg/dL) (n.v. < 1.0)	1.5 ± 3.0	3.6 ± 5.3	.054
Albumin (g/dL) (n.v. > 3.5)	4.3 ± 0.9	3.6 ± 0.9	.011 (.036)
Prothrombin time (INR) (n.v. < 1.2)	1.03 ± 0.16	1.13 ± 0.20	.109
Ascites (n)	19 (12%)	3 (30%)	.125
Mayo score	5.6 ± 1.4	6.9 ± 1.9	.011 (.015)

NOTE. Continuous variables are expressed as the mean ± SD. Only P values below .2 for the comparison between patient groups are reported before and after correction for age and disease duration.

Abbreviations: NS, not significant; INR, international normalized ratio; n.v., normal value.

(14%) were homozygous T/T, and 71 (43%) were heterozygous C/T. No significant differences in genotype distribution were observed between patients and controls nor between patients with early and advanced disease. Similarly, no significant differences were found in the clinical features of patients with different genotypes (data not shown).

The PXR A7635G genotypes and allele frequencies among patients with PBC and controls are shown in Table 5. Twenty-eight (28%) of 100 patients with PBC were found to be homozygous A/A, 19 (19%) were homozygous G/G, and 53 (53%) were heterozygous A/G. This genotype distribution was similar to what was observed among controls. Patients with PBC presented similar clinical characteristics across the three genotypes (data not shown).

The PXR C8055T genotypes and allele frequencies among patients with PBC and controls are shown in Table 5. No significant differences were observed between patients and controls in the frequencies of C8055T genotypes nor between patients with early and advanced disease. When the clinical characteristics of patients with PBC were analyzed according to their PXR genotypes,

similar features were encountered in all groups (data not shown).

Discussion

We investigated several key SNPs of CYP2D6, CYP2E1, MDR1, and PXR in patients with PBC and geographically and sex-matched controls to determine if particular alleles contribute to a link between xenobiotics and PBC. We did not identify an association between such alleles and PBC. In addition, we correlated the genotypes of the investigated genes with histological stages and other clinical and biochemical features of patients in a cross-sectional fashion and identified a significant association of the frequency of CYP2E1 c2 allele with PBC severity. Our series, one of the largest series of PBC cases ever genotyped for candidate genes, included an unusually high frequency of AMA-negative patients, but in all cases the diagnosis was verified as described herein. Moreover, data from AMA-negative patients were similar to the AMA-positive group. Indeed, our comparisons (between patients and controls as well as among affected individuals) should therefore be regarded as statistically powerful.

Table 5. Distribution of PXR Genotypes and Alleles in Patients With PBC and Controls

	Controls	PBC		
		Total	Early Disease	Advanced Disease
-24385 C/C	76/225 (34%)	72/167 (43%)	36/77 (47%)	36/90 (40%)
-24385 C/T	119/225 (53%)	71/167 (43%)	31/77 (40%)	40/90 (44%)
-24385 T/T	30/225 (13%)	24/167 (14%)	10/77 (13%)	14/90 (16%)
-24385 T allele frequency	0.397	0.356	0.331	0.378
7635 A/A	32/102 (31%)	28/100 (28%)	12/42 (29%)	16/58 (28%)
7635 A/G	49/102 (49%)	53/100 (53%)	25/42 (59%)	28/58 (48%)
7635 G/G	20/102 (20%)	19/100 (19%)	5/42 (12%)	14/58 (24%)
7635 G allele frequency	0.436	0.455	0.417	0.483
8055 C/C	66/102 (65%)	63/99 (63%)	29/43 (68%)	34/56 (61%)
8055 C/T	29/102 (28%)	34/99 (34%)	13/43 (30%)	21/56 (37%)
8055 T/T	7/102 (7%)	2/99 (2%)	1/43 (2%)	1/56 (2%)
8055 T allele frequency	0.211	0.192	0.174	0.205

PBC has a wide spectrum of disease progression—some patients remain asymptomatic for decades after diagnosis, while others present a rapidly progressing disease leading to orthotopic liver transplantation or death. Although a number of genetic factors have been proposed to explain such differences, results obtained thus far have proven to be weak or limited to specific geographical areas.^{4,5,30,31}

Four CYP2D6 alleles (CYP2D6*3, CYP2D6*4, CYP2D6*5, and CYP2D6*6) are known to account for 93% to 97% of PM cases,⁷ with CYP2D6*4 alone accounting for approximately 75% of these^{10,32}; this is the most widely studied allele in association studies. Brown et al.⁸ demonstrated a link between the CYP2D6*4 allele and ankylosing spondylitis and postulated that the poor metabolism of xenobiotics by a defective CYP2D6 polymorphism might explain this association. Others have suggested that a PM state might increase susceptibility to Parkinson's disease because of impaired detoxification of neurotoxins.³³ It is interesting to note that patients with CYP2D6*4 had slight signs of more severe clinical features as indicated by the prevalence of ascites, though differences in other variables (e.g., total bilirubin) did not reach statistical significance. The low or null allelic frequencies observed for CYP2D6*3, CYP2D6*5, and CYP2D6*6 in a preliminary study performed on both patients and controls did not provide sufficient statistical power and did not warrant further investigation. It is important to note that the observed allelic frequencies are similar to previous reports for all the CYP2D6 polymorphisms studied herein.³⁴

CYP2E1 is involved in the metabolism of drugs, chemicals (including ethanol), and carcinogens, and its c1/c2 polymorphism has been shown to influence enzyme activity *per se*¹⁶ or when induced by specific agents.^{17,18} Interestingly, Tsutsumi et al.³⁵ demonstrated that the c2 allele is associated with the development of alcoholic liver disease, likely through the reduced observed activity.¹⁶ Conversely, subjects with the c1/c1 genotype had higher CYP2E1 activity induced by isoniazid, suggesting an association between such a genotype and susceptibility to antituberculosis drug-induced hepatitis.¹⁸ We can assume that the c1/c2 SNP is involved in determining CYP2E1 activity possibly induced by specific agents, thus influencing the clinical manifestations of several diseases.^{18,35-37} Many CYP2E1 substrates have been identified, including halothane, isoniazid, acetone, acetonitrile, estrogen metabolites, and ethanol. Halothane is of great interest in the association of xenobiotic metabolism and susceptibility to PBC, because the sera of patients with halothane-induced hepatitis have autoantibodies to the pyruvate dehydrogenase complex similar to PBC sera.¹³ Moreover, previous data have also indicated that both oxidative and reductive

metabolism of halothane can lead to active xenobiotics *in vivo*.² On the other hand, the influence of low doses of nicotine on the expression of liver CYP2E1 in animal models³⁸ is also interesting considering that smoking is a risk factor for PBC.¹⁴

The frequency of the c1/c2 genotype in patients with advanced stage PBC was significantly higher than that of early-stage PBC. Accordingly, among other variables, the Mayo score values in patients carrying the c2 allele were significantly higher than those observed in patients with the c1/c1 genotype. A possible confounding effect of age (one of the factors in the calculation of such prognostic index) or disease duration was considered in this comparison, and we also note that these variables were not significantly different in patients with different genotypes. Our results indicate that genetically determined alterations of the metabolism of xenobiotics possibly mediated by other compounds might play a role in determining disease severity. Interestingly, in one of our previous studies, AMA from patients with PBC often reacted with a higher titer against the xenobiotically modified peptide than with the native lipoyl domain; that is, altered lipoic acid actually increased antibody binding.² Considering such data and the results described herein, we hypothesize that higher CYP2E1 activity induced by the presence of the c2 allele may make patients with PBC produce more active xenobiotics, including drugs, resulting in an enhanced T-cell reactivity to organic modified autoepitopes. Although our findings on the CYP2E1 c2 allele were limited to a small subgroup of patients, this polymorphism in PBC should be further assessed as a prognostic marker. Our data therefore support the previously suggested hypothesis, derived from the weak association between PBC and human leukocyte antigen haplotypes,³⁹ that susceptibility and progression are most likely caused by a combination of several factors, including more than one genetic determinant (e.g., abnormalities in sex chromosomes⁴⁰) together with specific genomic variations.

The MDR1 gene is responsible for the production of PGP, which is highly expressed in intestinal epithelial cells, and its genetic polymorphisms play a major role in determining local defense against bacteria and xenobiotics.⁴¹ Individuals carrying the homozygous MDR1 3435TT genotype had on average a two-fold lower intestinal level of PGP expression compared with the CC genotype, resulting in decreased transport of PGP substrates into the gut lumen and higher absorption from the gastrointestinal tract.²⁰ We have postulated that xenobiotic modification of lipoic acid occurs on microbial proteins.⁴² In particular, we reported that sera from patients with PBC react in a highly directed and specific fashion against proteins from the ubiquitous xenobiotic-metabolizing

bacterium *Novosphingobium aromaticivorans*.⁴³ In the data presented herein, homozygous TT genotype was found in 20% of patients with PBC, and no significant differences were observed between patients and controls in the frequencies of MDR1 genotypes and alleles (T allele frequency 0.461 in patients with PBC vs. 0.488 in controls). In the future, studies designed to investigate MDR1 genetic polymorphisms linked to alterations in PGP expression or SNPs of other genes related to gastrointestinal protection against bacteria and xenobiotics should be addressed. Based on a similar hypothesis, we note that Pauli-Magnus et al.⁴⁴ recently investigated the genetic polymorphisms of two different adenosine triphosphate-dependent binding cassettes (ABC B11 and B6, or MDR3) and reported a lack of correlation between polymorphisms of such genes and susceptibility to PBC.

PXR is a nuclear hormone receptor that acts as a xenobiotic sensor to transcriptionally regulate many important genes such as CYP3A4 and MDR1. Although there is the extent of CYP3A4 phenotypic variation, few allelic polymorphisms with altered activity have been reported.⁴⁵ Functional genetic variations in PXR, on the other hand, influence the expression of CYP3A4.²² Among PXR SNPs, C-25385T was associated with CYP3A4 inducibility phenotype in the liver, while A7635G and C8055T were involved in intestinal CYP3A induction. In particular, 3A4 is the most abundant CYP detectable in the liver (18.4% of the total CYP activity) and that an increased CYP3A4 induction in the liver is associated with the PXR -25385CC genotype.⁴⁶ We postulate that higher liver CYP3A4 activity in patients with PBC directly caused by the PXR -25385 CC genotype may alter the metabolism of xenobiotics, thus leading to the induction of autoimmunity through the enhanced production of xenobiotic structural analogues of lipoic acid. Our data, however, showed that the frequency of the latter genotype among patients with PBC was not significantly different compared with matched controls (43% vs. 33%; $P = .06$). Similarly, no differences were observed in the prevalence of A7635G and C8055T genotypes. Because PBC presents a striking female predominance,²³ it is interesting to note that progesterone is one of the substrates of CYP3A4.⁴⁷

In summary, we concentrated on genes for which sound evidence has suggested characteristics constituting a possible link with PBC. Second, we note that our design allowed to investigate the crucial steps of xenobiotic transport and metabolism. Third, we chose variations within such genes that were demonstrated to be "coding" for phenotypic differences, although in the case of CYP2E1 such differences can be mediated by other compounds.

Our findings herein, along with our previous data, point toward a "multi-hit" pathogenesis of PBC, with different genetic factors leading to onset and severity of disease.

References

1. Long SA, Van de Water J, Gershwin ME. Antimitochondrial antibodies in primary biliary cirrhosis: the role of xenobiotics. *Autoimmun Rev* 2002;1:37-42.
2. Long SA, Quan C, Van de Water J, Nantz MH, Kurth MJ, Barsky D, et al. Immunoreactivity of organic mimeotopes of the E2 component of pyruvate dehydrogenase: connecting xenobiotics with primary biliary cirrhosis. *J Immunol* 2001;167:2956-2963.
3. Leung PS, Quan C, Park O, Van de Water J, Kurth MJ, Nantz MH, et al. Immunization with a xenobiotic 6-bromohexanoate bovine serum albumin conjugate induces antimitochondrial antibodies. *J Immunol* 2003;170:5326-5332.
4. Agarwal K, Jones DE, Bassendine MF. Genetic susceptibility to primary biliary cirrhosis. *Eur J Gastroenterol Hepatol* 1999;11:603-606.
5. Donaldson PT. Immunogenetics in liver disease. *Baillieres Clin Gastroenterol* 1996;10:533-549.
6. Powell JJ, Van de Water J, Gershwin ME. Evidence for the role of environmental agents in the initiation or progression of autoimmune conditions. *Environ Health Perspect* 1999;107(Suppl 5):667-672.
7. Zanger UM, Raimundo S, Eichelbaum M. Cytochrome P450 2D6: overview and update on pharmacology, genetics, biochemistry. *Naunyn Schmiedebergs Arch Pharmacol* 2004;369:23-37.
8. Brown MA, Edwards S, Hoyle E, Campbell S, Laval S, Daly AK, et al. Polymorphisms of the CYP2D6 gene increase susceptibility to ankylosing spondylitis. *Hum Mol Genet* 2000;9:1563-1566.
9. Meyer UA, Skoda RC, Zanger UM. The genetic polymorphism of debrisoquine/sparteine metabolism-molecular mechanisms. *Pharmacol Ther* 1990;46:297-308.
10. Sachse C, Brockmoller J, Bauer S, Roots I. Cytochrome P450 2D6 variants in a Caucasian population: allele frequencies and phenotypic consequences. *Am J Hum Genet* 1997;60:284-295.
11. Lieber CS. Cytochrome P-4502E1: its physiological and pathological role. *Physiol Rev* 1997;77:517-544.
12. Selmi C, Invernizzi P, Miozzo M, Podda M, Gershwin ME. Primary biliary cirrhosis: does X mark the spot? *Autoimmun Rev* (in press).
13. Christen U, Quinn J, Yeaman SJ, Kenna JG, Clarke JB, Gandolfi AJ, et al. Identification of the dihydrolipoamide acetyltransferase subunit of the human pyruvate dehydrogenase complex as an autoantigen in halothane hepatitis. Molecular mimicry of trifluoroacetyl-lysine by lipoic acid. *Eur J Biochem* 1994;223:1035-1047.
14. Parikh-Patel A, Gold EB, Worman H, Krivy KE, Gershwin ME. Risk factors for primary biliary cirrhosis in a cohort of patients from the united states. *HEPATOLOGY* 2001;33:16-21.
15. Agundez JA. Cytochrome p450 gene polymorphism and cancer. *Curr Drug Metab* 2004;5:211-224.
16. Marchand LL, Wilkinson GR, Wilkens LR. Genetic and dietary predictors of CYP2E1 activity: a phenotyping study in Hawaii Japanese using chlorzoxazone. *Cancer Epidemiol Biomarkers Prev* 1999;8:495-500.
17. Lucas D, Menez C, Girre C, Berthou F, Bodenez P, Joannet I, et al. Cytochrome P450 2E1 genotype and chlorzoxazone metabolism in healthy and alcoholic Caucasian subjects. *Pharmacogenetics* 1995;5:298-304.
18. Huang YS, Chern HD, Su WJ, Wu JC, Chang SC, Chiang CH, et al. Cytochrome P450 2E1 genotype and the susceptibility to antituberculosis drug-induced hepatitis. *HEPATOLOGY* 2003;37:924-930.
19. Hoffmeyer S, Burk O, von Richter O, Arnold HP, Brockmoller J, Johne A, et al. Functional polymorphisms of the human multidrug-resistance gene: multiple sequence variations and correlation of one allele with P-glycoprotein expression and activity in vivo. *Proc Natl Acad Sci U S A* 2000;97:3473-3478.

20. Schwab M, Schaeffeler E, Marx C, Fromm MF, Kaskas B, Metzler J, et al. Association between the C3435T MDR1 gene polymorphism and susceptibility for ulcerative colitis. *Gastroenterology* 2003;124:26–33.
21. Glas J, Torok HP, Schiemann U, Folwaczny C. MDR1 gene polymorphism in ulcerative colitis. *Gastroenterology* 2004;126:367.
22. Zhang J, Kuehl P, Green ED, Touchman JW, Watkins PB, Daly A, et al. The human pregnane X receptor: genomic structure and identification and functional characterization of natural allelic variants. *Pharmacogenetics* 2001;11:555–572.
23. Kaplan MM. Primary biliary cirrhosis. *N Engl J Med* 1996;335:1570–1580.
24. Kaplan MM. Primary biliary cirrhosis: past, present, and future. *Gastroenterology* 2002;123:1392–1394.
25. Ludwig J, Dickson ER, McDonald GS. Staging of chronic nonsuppurative destructive cholangitis (syndrome of primary biliary cirrhosis). *Virchows Arch A Pathol Anat Histol* 1978;379:103–112.
26. Dickson ER, Grambsch PM, Fleming TR, Fisher LD, Langworthy A. Prognosis in primary biliary cirrhosis: model for decision making. *HEPATOLOGY* 1989;10:1–7.
27. Schaeffeler E, Schwab M, Eichelbaum M, Zanger UM. CYP2D6 genotyping strategy based on gene copy number determination by TaqMan real-time PCR. *Hum Mutat* 2003;22:476–485.
28. Choi JY, Lee KM, Cho SH, Kim SW, Choi HY, Lee SY, et al. CYP2E1 and NQO1 genotypes, smoking and bladder cancer. *Pharmacogenetics* 2003;13:349–355.
29. Cascorbi I, Gerloff T, John A, Meisel C, Hoffmeyer S, Schwab M, et al. Frequency of single nucleotide polymorphisms in the P-glycoprotein drug transporter MDR1 gene in white subjects. *Clin Pharmacol Ther* 2001;69:169–174.
30. Selmi C, Zuin M, Biondi ML, Invernizzi P, Battezzati PM, Bernini M, et al. Genetic variants of endothelial nitric oxide synthase in patients with primary biliary cirrhosis: association with disease severity. *J Gastroenterol Hepatol* 2003;18:1150–1155.
31. Tanaka A, Quaranta S, Mattalia A, Coppel R, Rosina F, Manns M, et al. The tumor necrosis factor- α promoter correlates with progression of primary biliary cirrhosis. *J Hepatol* 1999;30:826–829.
32. Daly AK, Armstrong M, Monkman SC, Idle ME, Idle JR. Genetic and metabolic criteria for the assignment of debrisoquine 4-hydroxylation (cytochrome P4502D6) phenotypes. *Pharmacogenetics* 1991;1:33–41.
33. McCann SJ, Pond SM, James KM, Le Couteur DG. The association between polymorphisms in the cytochrome P-450 2D6 gene and Parkinson's disease: a case-control study and meta-analysis. *J Neurol Sci* 1997;153:50–53.
34. Griese EU, Zanger UM, Bruderhans U, Gaedigk A, Mikus G, Morike K, et al. Assessment of the predictive power of genotypes for the in-vivo catalytic function of CYP2D6 in a German population. *Pharmacogenetics* 1998;8:15–26.
35. Tsutsumi M, Takada A, Wang JS. Genetic polymorphisms of cytochrome P4502E1 related to the development of alcoholic liver disease. *Gastroenterology* 1994;107:1430–1435.
36. Guengerich FP, Shimada T. Activation of procarcinogens by human cytochrome P450 enzymes. *Mutat Res* 1998;400:201–213.
37. Maezawa Y, Yamauchi M, Toda G. Association between restriction fragment length polymorphism of the human cytochrome P45011E1 gene and susceptibility to alcoholic liver cirrhosis. *Am J Gastroenterol* 1994;89:561–565.
38. Howard LA, Micu AL, Sellers EM, Tyndale RF. Low doses of nicotine and ethanol induce CYP2E1 and chlorzoxazone metabolism in rat liver. *J Pharmacol Exp Ther* 2001;299:542–550.
39. Tanaka A, Borchers AT, Ishibashi H, Ansari AA, Keen CL, Gershwin ME. Genetic and familial considerations of primary biliary cirrhosis. *Am J Gastroenterol* 2001;96:8–15.
40. Invernizzi P, Miozzo M, Battezzati PM, Bianchi I, Grati FR, Simoni G, et al. Frequency of monosomy X in women with primary biliary cirrhosis. *Lancet* 2004;363:533–535.
41. Thiebaut F, Tsuruo T, Hamada H, Gottesman MM, Pastan I, Willingham MC. Cellular localization of the multidrug-resistance gene product P-glycoprotein in normal human tissues. *Proc Natl Acad Sci U S A* 1987;84:7735–7738.
42. Van de Water J, Ishibashi H, Coppel RL, Gershwin ME. Molecular mimicry and primary biliary cirrhosis: premises not promises. *HEPATOLOGY* 2001;33:771–775.
43. Selmi C, Balkwill DL, Invernizzi P, Ansari AA, Coppel RL, Podda M, et al. Patients with primary biliary cirrhosis react against a ubiquitous xenobiotic-metabolizing bacterium. *HEPATOLOGY* 2003;38:1250–1257.
44. Pauli-Magnus C, Kerb R, Fattinger K, Lang T, Anwald B, Kullak-Ublick GA, et al. BSEP and MDR3 haplotype structure in healthy Caucasians, primary biliary cirrhosis and primary sclerosing cholangitis. *HEPATOLOGY* 2004;39:779–791.
45. Sata F, Sapone A, Elizondo G, Stocker P, Miller VP, Zheng W, et al. CYP3A4 allelic variants with amino acid substitutions in exons 7 and 12: evidence for an allelic variant with altered catalytic activity. *Clin Pharmacol Ther* 2000;67:48–56.
46. Edwards RJ, Adams DA, Watts PS, Davies DS, Boobis AR. Development of a comprehensive panel of antibodies against the major xenobiotic metabolising forms of cytochrome P450 in humans. *Biochem Pharmacol* 1998;56:377–387.
47. Lewis DF. Structural characteristics of human P450s involved in drug metabolism: QSARs and lipophilicity profiles. *Toxicology* 2000;144:197–203.

c-JUN NH₂-TERMINAL KINASE PATHWAY IS INVOLVED IN CONSTITUTIVE MATRIX METALLOPROTEINASE-1 EXPRESSION IN A HEPATOCELLULAR CARCINOMA-DERIVED CELL LINE

Yoshihiko SUGIOKA, Tetsu WATANABE*, Yutaka INAGAKI, Miwa KUSHIDA, Maki NIIOKA, Hitoshi ENDO, Reichi HIGASHIYAMA and Isao OKAZAKI

Department of Community Health, Tokai University School of Medicine, Kanagawa, Japan

Transcription factor c-Jun serves for cellular proliferation, survival, differentiation and transformation and is recognized as an important factor in cancer development, including hepatocellular carcinoma (HCC). The purpose of present study is to determine the involvement of c-Jun in matrix metalloproteinase-1 (MMP-1) expression, which is previously reported by us to be expressed only in the early stage of human HCC showing stromal invasion. Of 5 human HCC cell lines examined, only HLE cells revealed mRNA and protein expression as well as enzymatic activity of MMP-1. Transient transfection of an MMP-1 promoter/luciferase construct (including 4.4 kb full promoter region) into HLE and HCC-T cells (MMP-1 nonproducer) showed that high promoter activity was observed only in HLE cells without inducers, and that this promoter activity was still observed when a shorter 0.6 kb proximal promoter construct was transfected. The 0.6 kb promoter region contained 3 AP-1 sites, and c-jun mRNA was constitutively expressed in HLE cells without inducers. Furthermore, phosphorylated c-Jun and c-Jun NH₂-terminal kinase (JNK) were detected in HLE cells. Promoter activity of the 0.6 kb construct was suppressed with SP600125, a potent inhibitor of JNK, but not with PD98059 and SB203580, potent inhibitors of MEK1/2 and p38, respectively. The inhibitory effect of SP600125 was also observed at protein expression level and in enzymatic activity of MMP-1. Taken together, this study suggests that the JNK pathway is involved in the expression of MMP-1 in HCC cells and may represent a new functional role of c-Jun for HCC development.

© 2004 Wiley-Liss, Inc.

Key words: hepatocellular carcinoma; matrix metalloproteinase-1; c-Jun; MAP kinase inhibitors; JNK pathway

Invasion and metastasis are the major causes of treatment failure in patients with cancer. Enzymatic degradation of different macromolecular components of the extracellular matrix (ECM), which is an essential step in the process of invasion and metastasis, plays a key role in the dissemination of cancer cells.^{1,2} Of several proteolytic enzymes, it has been clarified that metalloproteinases (MMPs) are responsible for ECM destruction, and that they participate in cancer cell invasion and metastasis.^{3,4}

We previously showed that only well-differentiated cancer cells of early hepatocellular carcinoma (HCC), smaller than 2 cm in diameter, express matrix metalloproteinase-1 (MMP-1) by *in situ* hybridization and immunohistochemistry.⁵ Early HCC is usually described as well-differentiated carcinoma⁶ and stromal invasion of cancer cells is a common finding in early HCC.⁷ As HCC is usually associated with liver fibrosis/cirrhosis,^{8–10} where type 1 collagen is mainly deposited, it is quite likely that early HCC cells invade surrounding fibrous tissue by secreting MMP-1. MMP-1 expression is only detected in the early stage of HCC, which is coincident with clinical feature of HCC. In advanced stage of HCC, they are usually encapsulated with fibrous tissue and invade surrounding fibrous tissues no longer.

A recent study revealed that MMP-2 and membrane type 1-matrix metalloproteinase (MT1-MMP) can cause the cells to proliferate¹¹ besides their well-known original function, that is, ECM resolution. Moreover, MT1-MMP was reported to increase cell mobility.¹² MMP-1 was also supposed to cause the proliferation of

hepatocytes in the rat fibrotic liver infected with recombinant adenovirus harboring human MMP-1 gene.¹³

c-Jun and activated c-Jun by a phosphorylation cascade of mitogen-activated protein kinase (MAPK) families have been shown to play an important role in embryonic cell differentiation, apoptosis and proliferation as well as carcinogenesis of hepatocytes.¹⁴ The phosphorylation of c-Jun is conducted by c-Jun NH₂-terminal kinases (JNK) among 4 distinctly regulated groups of MAPK pathways; the other 3 groups are extracellular signal-related kinases (ERK)-1/2, p38 proteins and ERK5.^{15–18}

Several recent studies describing involvement of c-Jun in the early stage of HCC development¹⁴ or in liver regeneration after partial hepatectomy¹⁹ remind us that JNK pathway has a key role in the MMP-1 gene expression in HCC. MMP-1 gene expression is truly known to be regulated by c-Jun, but the regulation of MMP-1 gene expression by JNK pathway in HCC cells remains unknown. The present study has shown for the first time that one HCC cell line, which constitutively expresses MMP-1 without any stimulators such as phorbol ester, is under control of transcriptional regulation of the MMP-1 gene transcription via the activation of c-Jun through JNK pathway. These results may indicate an additional functional role of c-Jun in HCC development.

MATERIAL AND METHODS

HCC cell lines

Human HCC cell lines HLE,²⁰ PLC/PRF/5²¹ and Huh-7²² were obtained from the Japanese Cancer Research Resources Bank (Osaka, Japan). HCC-M and HCC-T were previously established by us.^{23,24} HCC-M, HLE, PLC/PRF/5 and Huh-7 were cultured in DMEM supplemented with 10% fetal bovine serum (FBS), non-essential amino acids and antibiotics. HCC-T was cultured with RPMI-1640 containing 10% FBS and antibiotics.

Reagents

c-Jun NH₂-terminal kinase inhibitor SP600125 was purchased from Calbiochem-Novabiochem (San Diego, CA). MEK/ERK inhibitor PD98059 and p38 inhibitor SB203580 were obtained from Sigma Chemical (St. Louis, MO).

RNA isolation and RT-PCR

Isolation of total RNA and RT-PCR were performed as described previously.²⁵ To amplify each gene, a pair of sense and antisense primers (Table I) were chosen with the help of a computer program (Oligo 5.0, Primer analysis software, National Bio-

*Correspondence to: Department of Community Health, Tokai University School of Medicine, Bohseidai, Isehara, Kanagawa, 259-1193, Japan. Fax: +81-463-92-3549. E-mail: tewatana@is.icc.u-tokai.ac.jp

Received 2 July 2003; Revised 9 October 2003; Accepted 27 November 2003

DOI 10.1002/ijc.20095

Published online 5 February 2004 in Wiley InterScience (www.interscience.wiley.com).

TABLE I - PRIMERS FOR RT-PCR AMPLIFICATION

Gene		Nucleotide sequence	Annealing temperature (°C)	Cycle	Product (bp)
Albumin	Sense	5'-CCCGGAACTCCTTTTCTTTG-3'	56	40	675
	Antisense	5'-CATCGAACACTTTGGCATAGCA-3'			
HNF-4	Sense	5'-CTGCTCGGAGCCACAAAGAGATCCATG-3'	57	30	371
	Antisense	5'-ATCATCTGCCACGTCATGCTCTGCA-3'			
AFP	Sense	5'-CGCTGGAACGTCGTCATGTA-3'	56	40	706
	Antisense	5'-CACCTGAGCTTGGCACAGA-3'			
MMP-1	Sense	5'-GGTGCCAGTGCTTGAATAAT-3'	57	35	716
	Antisense	5'-CATCACTTCTCCCGAATCGT-3'			
MMP-2	Sense	5'-TCTTCCCTCGCAAGCCCAACT-3'	57	35	685
	Antisense	5'-ACAGTGGACATGGCGGTCTCAG-3'			
MMP-9	Sense	5'-TGGGTACGTGACCTATGAC-3'	59	35	200
	Antisense	5'-CAAAGGTGAGAAGAGAGGGC-3'			
TIMP-1	Sense	5'-TTCTGCAATTCCGACCTCGTC-3'	58	30	385
	Antisense	5'-GCACTTTGCAGGGGATGGATA-3'			
c-jun	Sense	5'-CCTGTTGCGGCCCGAAACT-3'	62	30	495
	Antisense	5'-ACCATGCTGCCCGTTGAC-3'			
c-fos	Sense	5'-TTGCCTAACCGCCACGATGAT-3'	62	30	500
	Antisense	5'-TTGCCGCTTCTGCCACCTC-3'			
G3PDH	Sense	5'-ACCACAGTCCATGCCATCAC-3'	62	23	452
	Antisense	5'-TCCACCACCCTGTGCTGTA-3'			

science, Plymouth, MN). Each target gene was amplified in the GeneAmp PCR System 9600 (Perkin Elmer, Norwalk, CT). The initial denaturation was at 94°C for 2 min, followed by each cycle of reaction at 94°C for 30 sec, at the described annealing temperature for 30 sec (Table I), and at 72°C for 30 sec, and followed by postextension at 72°C for 7 min. Glyceraldehyde 3-phosphate dehydrogenase (G3PDH), which was used as an internal control, was amplified for 23 cycles as previously described.²⁵ The PCR products were separated by electrophoresis on a 1.5% agarose gel, stained with ethidium bromide.

Zymography

To examine the gelatinolytic activity, gelatin zymography was performed as described before²⁵ with a slight modification. After cells were cultured in serum-free media for 48 hr, aliquots of the culture media from HCC cells were mixed with 4 × gel loading buffer (10% SDS, 4% sucrose, 0.25 M Tris-HCl, pH 6.8, 0.1% bromophenol blue) without boiling, then electrophoresed on a 10% polyacrylamide gel containing 1 mg/mL of gelatin. The volume of media loaded was adjusted according to the cell number. Gels were scanned in a digital scanner and densitometric measurement was performed with NIH Image software (version 1.55).

Nucleotide sequence analysis for single nucleotide polymorphism at -1607 bp

To detect the known 1G/2G polymorphism at -1607 bp in the MMP-1 promoter region, PCR amplification was performed with a pair of primers, M-F (5'-ACATGTTATGCCACTTAGAT-3'; -1654/-1635) and M-R (5'-TCCCCTTATATGGATTCCGTGTT-3'; -1536/-1517), followed by nucleotide sequence analysis.²⁶

Plasmid constructs

A fragment encompassing the essential sequence for transcriptional activity of MMP-1 promoter was amplified from genomic DNA isolated from HCC-T cells using the following primers: sense, 5'-TTTCAAATCCATCTCAAATTCACA-3' (-4363/-4340); antisense, 5'-ACTGGCCTTGTCTCTTCTCAG-3' (+49/+72). *Bgl*II digestion of the resulting 4,429 bp PCR product (-4363/+72; 4.4 kb construct) yielded a 1.2 kb fragment (-1196/+72), which was cloned into the pGL3 Basic vector (Promega, Tokyo, Japan) that had been treated to have the same termini. A 5' deletion promoter 0.6 kb construct (-522/+72) was generated from this construct (-1196/+72) by using convenient restriction site (*Kpn*I at -517 bp). Those chimeric constructs were sequenced and found to be identical to the previously reported sequence²⁷ except that our sequence from HCC-T had a "T" at site -320 nucleotide, where the published sequence contained a "C" at that

site. Expression plasmid pCMV-jun was the kind gift of Dr. Tom Curran.

Transient transfection and assessment of promoter activity

The MMP-1 promoter/luciferase constructs were transfected into HLE and HCC-T cells using the calcium phosphate-DNA coprecipitation method. In some experiments, human MMP-1 promoter/luciferase reporter gene construct (-522/+72; 0.6 kb) was cotransfected with pCMV-jun expression vector into HCC-T cells. Total amount of transfected DNA was adjusted with pCMV empty vector. Transfection efficiency was normalized by using pRL-CMV vector (Promega) as an internal control. Five hours after transfection, the cells were treated with 15% glycerol for 105 sec, then incubated for 48 hr. Firefly and Renilla luciferase activities were measured using Dual-Luciferase Reporter Assay System (Promega). Cell transfections and luciferase assays were repeated independently more than 3 times, each performed in duplicate.

Western blot analysis for MMP-1 and phosphorylated c-Jun

For the detection of MMP-1, culture media described above were also used for Western blot analysis. The concentration of protein was measured with DC protein assay Kit (Bio-Rad, Richmond, CA). Samples were mixed with 4 × SDS sample buffer (0.25 M Tris-HCl, pH 6.8, 8% SDS, 20% glycerol, 5% β-mercaptoethanol) and equal amount of protein per lane was run on a 10% SDS-PAGE and transferred onto a PVDF membrane (Amersham Biosciences, Buckinghamshire, U.K.). Blots were incubated with anti-MMP-1 antibody (Daiichi Fine Chemical, Takaoka, Japan) at a dilution of 1:1,000 for 2 hr, followed by incubation with rabbit antimouse IgG second antibody (Dako, Glostrup, Denmark) at a dilution of 1:2,000 for 1 hr at room temperature. The proteins were visualized by chemiluminescence by using ECL Plus detection kit (Amersham Biosciences) according to the manufacturer's instruction. For the detection of phosphorylated c-Jun, PhosphoPlus c-Jun (Ser63) II and c-Jun (Ser73) Antibody Kit (Cell Signaling Technology, Beverly, MA) was used according to the manufacturer's instruction. For the confirmation of equal loading, blots were reprobated with anti-β-actin antibody (Sigma Chemical).

In vitro kinase assay

Phosphorylated JNK and total-JNK were detected with Fast Activated Cell-Based ELISA (FACE) JNK Kit (Active Motif North America, Carlsbad, CA) following manufacturer's instructions. Briefly, about 1,000 cells per well were seeded in 2 96-well plates as replicates and incubated for 48 hr and the cells were fixed. One plate was treated with the antiphospho-JNK antibody, while the other plate was treated with anti-JNK antibody. The relative

number of cells in each well was then determined through use of the Crystal Violet reagent. Once the phospho-JNK and total JNK signals were normalized for cell number, a comparison of the ratio of phosphorylated JNK to total JNK for each of the cell growth conditions was determined.

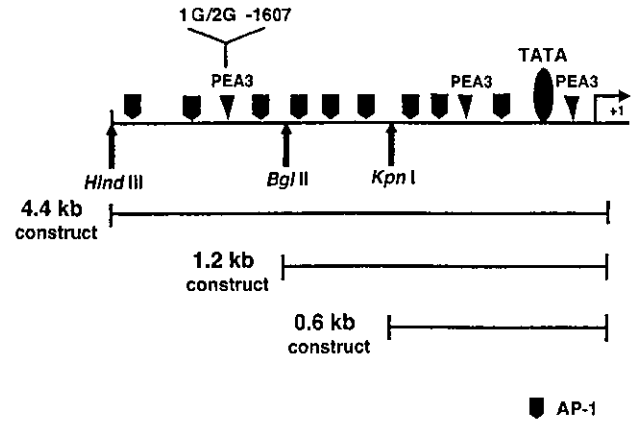
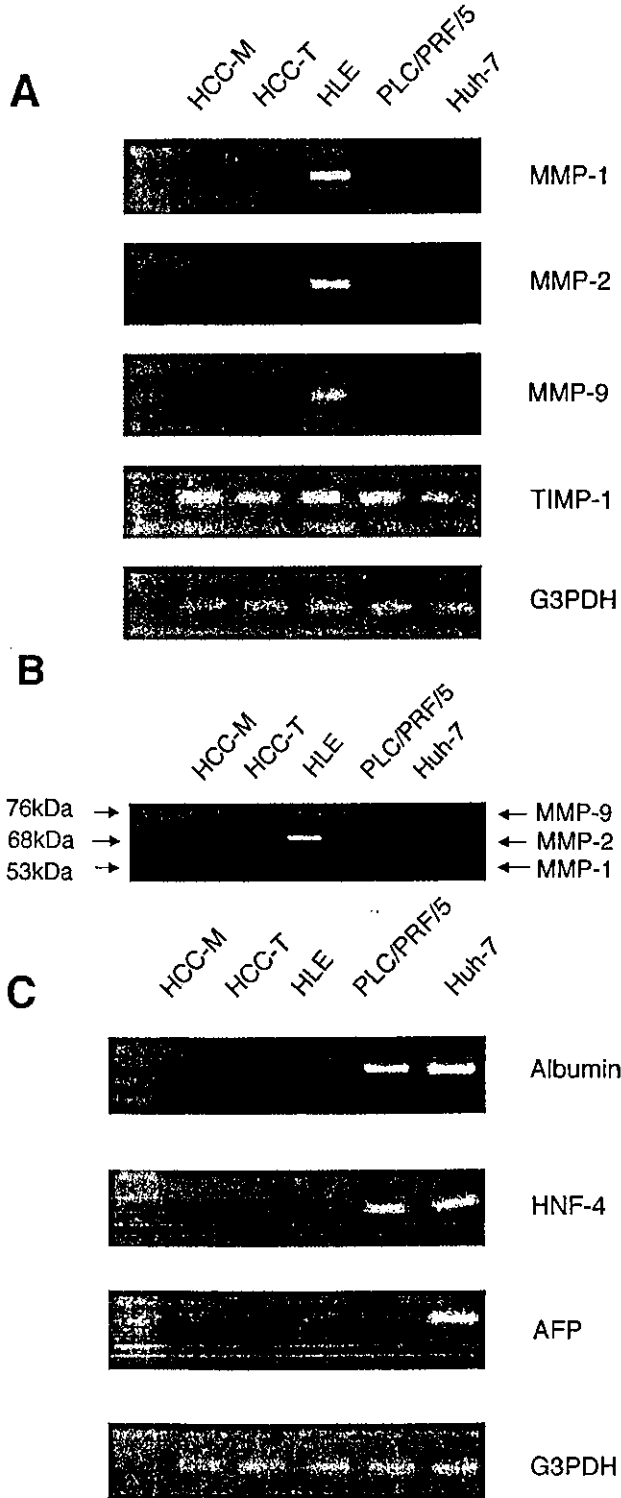


FIGURE 2—Schematic representation of human MMP-1 promoter constructs. Three convenient restriction sites, *HindIII*, *BglII* and *KpnI*, were used to generate the 4.4, 1.2 and 0.6 kb promoter constructs, which were transfected into HLE and HCC-T cells to determine the promoter activity. Three AP-1 sites, 2 PEA-3 sites and TATA box are included in the 0.6 kb promoter construct. The “Y” indicates functional polymorphism in MMP-1 promoter. The bent arrow represents the beginning of transcription. Modified from Benbow and Brinckerhoff.¹⁸

Statistical analysis

The data were expressed as mean ± standard deviation. Statistical analysis was performed using Mann-Whitney test. *p*-values less than 0.05 were considered statistically significant.

RESULTS

MMP-1 expression and cell marker characteristics in HCC cell lines

Among the HCC cell lines examined, definite expression of MMP-1, MMP-2 and MMP-9 mRNAs was found only in HLE cells, while these 3 MMPs were not detected in HCC-M and HCC-T cells (Fig. 1a). HCC-T and PLC/PRF/5 cells showed a slight positive transcription of MMP-2. TIMP-1 mRNA was expressed in all cell lines in the present study (Fig. 1a). Gelatin zymography revealed definite bands at 76, 68 and 53 kDa only in HLE cells, which corresponded to enzymatic activity of MMP-9, MMP-2 and MMP-1, respectively (Fig. 1b). The other 4 cell lines did not show any bands.

Five cell lines were established from patients with different differentiation stages of characteristics. Both PLC/PRF/5 and Huh-7 cells showed positive mRNAs of both albumin and HNF-4,

FIGURE 1—MMPs and TIMP-1 expression in HCC cell lines. (a) MMP-1, MMP-2, MMP-9 and TIMP-1 expressions in 5 HCC cell lines were detected by RT-PCR analysis. Total RNA was extracted from HCC cells and 1 µg of total RNA was used as a template as described in text. The strong bands of MMP-1, MMP-2 and MMP-9 were observed only in HLE cell line. HCC-T and PLC/PRF/5 cells showed a slight positive transcription of MMP-2. The expression of TIMP-1 was seen in every cell line. G3PDH (bottom) was used as an internal control. (b) Gelatin zymography of conditioned media from cultured 5 HCC cell lines. Semiconfluent HCC cells grown in 60 mm tissue culture plates were replaced with serum-free media and cells were cultured for a further 48 hr. Bands of negative staining indicated zones of enzyme activities. Gelatinolytic activity of MMP-1, MMP-2 and MMP-9, which corresponded to 53, 68 and 76 kDa bands, respectively, were seen only in HLE cells. (c) Cell marker characteristics in HCC cell lines. The expressions of albumin, HNF-4 and α-fetoprotein (AFP) were also assayed by RT-PCR analysis. The distinct albumin and HNF-4 mRNA was observed in PLC/PRF/5 and Huh-7 cells. The strong band of AFP was found in Huh-7 cells.